
Article:
Yao, L, Aretz, M, Wignall, PB orcid.org/0000-0003-0074-9129 et al. (5 more authors) (2020) The longest delay: Re-emergence of coral reef ecosystems after the Late Devonian extinctions. Earth-Science Reviews, 203. 103060. ISSN 0012-8252

https://doi.org/10.1016/j.earscirev.2019.103060

The longest delay: re-emergence of coral reef ecosystems after the Late Devonian extinctions

Le Yao[a,*], Markus Aretz[b], Paul B. Wignall[c], Jitao Chen[a], Daniel Vachard[d], Yuping Qi[a], Shuzhong Shen[e,a], Xiangdong Wang[e,a]

[a]*State Key Laboratory of Palaeobiology and Stratigraphy, Nanjing Institute of Geology and Palaeontology, and Center for Excellence in Life and Palaeoenvironment, Chinese Academy of Sciences, Nanjing 210008, China*

[b]*GET, Université de Toulouse, CNRS, IRD, UPS, Toulouse 31400, France*

[c]*School of Earth and Environment, University of Leeds, Leeds LS2 9JT, UK*

[d]*1, rue des Tilleuls, Gruson 59152, France*

[e]*School of Earth Sciences and Engineering, Nanjing University, Nanjing 210023, China*

*Correspondence should be addressed to Le Yao, Email: lyao@nigpas.ac.cn

Abstract

Reefs are an excellent tool for tracking marine-ecosystem changes, especially through mass extinction transitions. Although metazoan reefs proliferated during the Phanerozoic, prolonged metazoan reef-recovery intervals often occurred after extinction events. Here, we document and review the reef-recovery interval following the Late Devonian Frasnian-Famennian (Kellwasser) and end-Famennian (Hangenberg) mass extinctions, which eliminated the largest area of metazoan (stromatoporoid-coral) reefs of the Phanerozoic. Previous reports of the late Visean coral bioconstructions from western Palaeotethys Ocean, may mark the first metazoan reef proliferation after the Hangenberg extinction. In this study, abundant coral reefs, coral frameworks and coral biostromes were described in detail for the first time from the late Visean strata on the South China Block (eastern Palaeotethys Ocean). The occurrence of these coral bioconstructions further suggests that the late Visean coral reef recovery may have been a widespread phenomenon. Based on the high-resolution reef database constructed in this study, three sub-intervals of the Mississippian metazoan reef recovery were distinguished, which are (1) metazoan "reef gap" phase (MRG) without metazoan reefs during the Tournaisian; (2) metazoan reef re-establishment phase (MRR) containing a few metazoan reefs from early Visean to early part of the late Visean; and 3) metazoan reef proliferation phase (MRP) with global coral reef flourishment during the middle part of the late Visean (late Asbian to early Brigantian substages). Hence, coral reef ecosystems proliferated and became dominant in marine ecosystems during the late Asbian to early Brigantian, indicating a prolonged metazoan reef recovery of about 12 Ma and 23 Ma until the MRR and MRP, respectively. Coral reef proliferation at this time shows that the Mississippian was not solely a period dominated by microbial reefs. Late Visean coral reef development

coincided with increased nektonic and benthic diversity, showing that metazoan reef recovery closely tracked overall marine ecosystem evolution. Even compared with other slow reef-recovery intervals, such as the middle-late Cambrian and Early-Middle Triassic with the intervals until the MRR and MRP of 5 Ma and 2 Ma, and 15 and 9 Ma respectively, the Mississippian metazoan reef recovery was the longest in reef history. Harsh climatic and oceanic conditions were present during the Mississippian, mainly including the widespread marine anoxia during the middle part of Tournaisian and the following recurrent glacial and interglacial climatic episodes with frequent changes in sea level, sedimentary facies and sea-water surface temperature, which may have stymied metazoan reef recovery during this time. During the late Visean, marine communities flourished during a phase of relative warm conditions and high sea level, and coincided with the long-delayed re-emergence of coral reef ecosystems after the Late Devonian extinctions.

Keywords: Coral reef; diversity; recovery; mass extinction; glacial and interglacial climate; Mississippian

1. Introduction

Reefs typically form in shallow, tropical carbonate platforms, which are the cradle of evolution and sources of marine biodiversity (Kiessling et al., 2010). The earliest examples were formed of stromatolites and flourished during the Precambrian before declining in the Phanerozoic (Riding, 2006). Metazoan reefs first appeared in the late Ediacaran and proliferated during the Phanerozoic (Wood, 1999; Penny et al., 2014), albeit with time gaps after mass extinction events, which are often marked by microbial reef proliferation (Riding, 2006; Yao et al., 2016a).

The most persistent development of metazoan reef ecosystems occurred from the Ordovician to Devonian, when stromatoporoids and tabulate corals dominated (Copper, 2011; Zapalski et al., 2017a). It reached its climax during the Middle to Late Devonian (Givetian to Frasnian stages), when reefs covered about five million square kilometres (10 times the surface area of modern reef ecosystems) and had remarkable longitudinal extent (Copper, 1994; Copper and Scotese, 2003). This reef heyday was followed by the Famennian to Mississippian interval that saw the transition from Devonian greenhouse to Permo-Carboniferous icehouse climate (Montañez et al., 2011) and the Frasnian-Famennian (F-F) Kellwasser and end-Famennian Hangenberg mass extinction events (Hallam and Wignall, 1997; Kaiser et al., 2016). The F-F extinction caused the collapse of stromatoporoid-tabulate coral ecosystems, which were replaced by the early Famennian microbial reef ecosystems with a few stromatoporoid reefs (Copper, 2002). Then, the abundance of microbial and stromatoporoid reefs gradually declined until the latest Devonian when stromatoporoid reef ecosystems became dominant again only to be eliminated during the Hangenberg extinction (Webb, 2002; Yao et al., 2016a). The succeeding Mississippian has long been assumed to be an interval dominated by microbial reefs, containing a major metazoan "reef gap" (Heckel, 1974; Webb, 1994). Small-sized metazoan reefs gradually reappeared during the middle-late Mississippian (Visean Stage) (Webb, 2002; Aretz and Chevalier, 2007; Rodríguez et al., 2012; Yao and Wang, 2016). However, due to low-resolution and limited data available in previous studies (e.g. Webb, 2002), the timing and style of metazoan reef recovery in the Mississippian are unclear.

Evaluations of post-extinction marine ecosystems have focused primarily on the number of taxa, with less attention paid to ecological change (e.g., Poty, 1999; Song et al., 2011; Chen and

Benton, 2012). However, biodiversity metrics do not reveal all aspects of recovery, and an ecological approach is essential (Chen and Benton, 2012; McGhee et al., 2013), particularly for metazoan reef ecosystems (Yao et al., 2016a). Metazoan reef recoveries after mass extinctions often occur following major time gaps, such as the middle-late Cambrian, Mississippian and Early-Middle Triassic (Lee et al., 2015; Yao et al., 2016a; Martindale et al., 2018). The longest metazoan "reef gap" was during the Mississippian (Adachi et al., 2015; Yao et al., 2016a), but the biodiversity variations in this interval are poorly documented, as are the coeval climatic and environmental changes. Thus, the trajectory of Mississippian marine ecosystem recovery after the Late Devonian mass extinctions requires more detailed study. Thus, our main aims are: 1) to review the Mississippian bioconstructions from the Palaeotethys and Panthalassa oceans and to describe the coeval coral bioconstructions in detail from the South China Block; 2) to reconstruct a global Mississippian reef database at a high temporal resolution in order to constrain the duration and timing of metazoan reef proliferation; 3) to compare the Mississippian metazoan reef evolutionary pattern with contemporaneous diversity changes in marine nektonic and benthic faunas, and thus provide insight into the overall marine ecosystem changes; and 4) to discuss the potential factors controlling the prolonged Mississippian metazoan reef recovery.

2. Reef definition and synonymy

Reef is a controversial term with no consistent definition, due to the varying opinions of different researchers. Riding (2002) defines it as "calcareous deposits created by essentially in place sessile organisms", whilst Kiessling (2002) refers to a "laterally confined biogenic structure, developed by the growth or activity of sessile benthic organisms with topographic relief and

(inferred) rigidity". In this paper, we use Riding's broad definition, which we consider to be synonymous with bioconstruction (Aretz and Chevalier, 2007). According to the classifications of Kershaw (1994) and Flügel (2004), reef/bioconstruction types include organic reef (true reef as defined by Kiessling (2002)), reef mound, mud mound, and biostrome. Frameworks are meshworks with rigidity (Aretz and Chevalier, 2007), which contribute to form organic/true reefs (Flügel, 2004). Reef mound is defined as bioconstructions built by bioclastic lime mud with minor amounts of organic bindings forming frameworks (Flügel, 2004). Mud mounds consist of a high amount of fine-grained carbonate (generally more than 50% of rock volume) (Flügel, 2004). Organic reef, reef mound and mud mound are characterized by positive relief (Flügel, 2004), which differs from (usually smaller) biostromes that can be bedded reefs with no significant relief compared to their lateral extension (see autobiostromes in Kershaw, 1994). Due to the uncertain origin and the common deep-slope location of mud mounds (Riding, 2002), they are excluded from this study which focuses on bioconstructions formed in shallow-water carbonate platforms.

3. Geological setting

3.1. Palaeogeographic and geographic locations

During the Mississippian, the main palaeocontinents of Gondwana, Laurussia, Siberia, North and South China blocks, were separated by the Palaeotethys and Panthalassa oceans (Blakey, 2011; Fig. 1). Polar to temperate settings characterised much of southern Gondwana and Siberia, whereas most other landmasses and major parts of the Palaeotethys Ocean were in warm (temperate to tropical) settings. Due to the rotation and northward drift of Gondwana, the tropical seaway, parallel to the palaeoequator, between Laurussia and Gondwana closed during the late

Mississippian (Nance and Linnemann, 2008; Shen et al., 2016).

In this study, we compiled and reviewed the Mississippian reef sites of Europe and eastern Canada (southeastern Laurussia) and North Africa (northwestern Gondwana) in the western Palaeotethys Ocean, of southern Turkey (northern Gondwana) in the southern Palaeotethys Ocean, of western and central United States of America and western Canada (western Laurussia) in the eastern Panthalassa Ocean, and of eastern Australia (small terranes near the northeastern Gondwana), of Japan (seamount near the North China Block) and of northwestern China (eastern Tianshan orogenic belt between the Siberian and Tarim blocks) in the western Panthalassa Ocean (Domeier and Torsvik, 2014; Fig. 1). Extensive new reef data are added from the South China Block (SCB). They are from the Yashui section in Huishui County, Guizhou Province, and the Gandongzi and Xiadong sections in Tianlin County, Guangxi Province (Fig. 1D).

The SCB was located near the palaeoequator in northeastern Palaeotethys Ocean (Fig. 1). Compared to Mississippian times, it is today clockwise rotated by almost 90°. The marine realm of the SCB was highly differentiated into 1) nearshore siliciclastic facies bordering the Yangtze Old Land; 2) extensive shallow carbonate facies of the Dian-Qian-Gui-Xiang (DQGX) and Langping (LP) platforms; 3) the Qian-Gui (QG) basinal facies; 4) slope facies between the DQGX and LP platforms and the QG basin; and 5) deep-basin facies (Feng et al., 1998; Fig. 1D).

3.2. Chronostratigraphy and lithostratigraphy

The Mississippian chronostratigraphic and lithostratigraphic frameworks of the SCB were systematically reviewed, which include the following four stages of Tangbagouan, Jiusian, Shangsian and Dewuan from bottom to top, and various formations in different provinces (Hance

et al., 2011; Wang et al., 2019; Figs. 1D, 2). Abundant organic reefs and biostromes have been found in the Yashui area in Guizhou Province and in the Langping area in Guangxi Province (Fig. 2). In the Yashui area, there are five Mississippian formations: the Tangbagou, Xiangbai, Jiusi, Shangsi and Baizuo in ascending order. In the Langping area, two formations were distinguished: the Yaoyunling and Du' an, which are correlative with the Tangbagou and its overlying four formations combined, respectively (Hance et al., 2011; Wang et al., 2019; Fig. 2). In this study, the organic reefs and biostromes documented from South China, are in the upper Shangsi and middle Du'an formations (Fig. 2).

Stratigraphic correlation of chronostratigraphic units between the SCB and other reef-bearing regions, enables an age framework of reef evolution during the Mississippian to be established. The Tangbagouan Stage (Tournaisian Stage) is approximately equivalent to the Courceyan or Hastarian and Ivorian substages in Western Europe, and the Kinderhookian to middle Osagean stages in North America. The Jiusian Stage (early to middle middle Visean Stage) is approximately equivalent with the Chadian to middle Holkerian substages or Moliniacian to middle Livian substages in Western Europe, and upper Osagean to middle Meramecian stages in North America. The Shangsian Stage (upper middle to upper Visean Stage) is approximately equivalent to the upper Holkerian to Brigantian substages or upper Livian to Warnantian substages in Western Europe, and upper Meramecian to lower Chesterian stages in North America. The Dewuan Stage (Serpukhovian Stage) is approximately equivalent to Pendleian to Arnsbergian substages in Western Europe, and upper Chesterian Stage in North America (Somerville, 2008; Hance et al., 2011; Wang et al., 2019; Fig. 2).

3.3. Biostratigraphy

The age of the Mississippian reefs is mainly constrained by foraminifer biostratigraphy, especially in Western Europe and South China where 16 Mississippian foraminifer zones (MFZs) are recognized (Poty et al., 2006; Hance et al., 2011; Fig. 2). Foraminiferal studies on the formations in Yashui and Langping areas allow comparisons with the MFZs. The Tangbagou Formation (Yaoyunling Formation), Xiangbai Formation (basal Du'an Formation), Jiusi Formation (lower Du'an Formation), Shangsi Formation (middle Du'an Formation) and Baizuo Formation (upper Du'an Formation) are approximately equivalent to the MFZ 1 to MFZ 7, MFZ 7 to MFZ 9, MFZ 9 to MFZ 12, MFZ 12 to MFZ 15, and MFZ 16, respectively (Hance et al., 2011; Fig. 2). The occurrence of the organic reefs and biostromes in the upper Shangsi and middle Du'an formations, suggests that they are of late Visean age (Fig. 2).

The age of the bioconstructions from South China was constrained by detailed foraminiferal studies combined with coral occurrences. At Gandongzi, the coral and coral-microbial-bryozoan reefs of the Du'an Formation are of Visean age (Hance et al., 2011). Abundant foraminifers, found in both the reefs and their underlying and overlying strata, include the typical late Visean taxa *Cribrospira* sp., *Cribrostomum* sp., *Endothyra* aff. *pulchra*, *E.* aff. *spira*, *E.* ex gr. *similis*, *E.* ex gr. *prisca*, *E.* sp., *Endothyranopsis* ex gr. *compressa*, *E.* sp., *Eostaffella* cf. *mirifica*, *Koskinotextularia* sp., *Palaeotextularia* ex gr. *longiseptata*, *P.* sp., *Tetrataxis* cf. *dentata*, *T.* ex gr. *acuta*, *T.* ex gr. *palaeotrochus*, and *T.* sp. The occurrence of *Cribrostomum* sp., *Koskinotextularia* sp., *Palaeotextularia* ex gr. *longiseptata*, and *P.* sp., suggests that the reefs belong to the MFZ 14 to lower MFZ 15 (Poty et al., 2006). At Longfeng, a section which is only about 200 m from the Gandongzi section, rich foraminiferal assemblages include *Cribrospira* sp., *Cribrostomum*

lecomptei, *C.* sp., *Endothyra* sp., *Endothyranopsis* ex gr. *compressa*, *Eostaffella* sp., *Janischewskina* sp., *Omphalotis omphalota*，*O.* sp., and *Palaeotextularia* ex gr. *longiseptata*. They further confirm the late Visean age (MFZ 14-15) for the Gandongzi reefs. The appearance of *Janischewskina* sp., at 32.8 m height in the Longfeng section (equal to the interval of 55 m to 63 m in the Gandongzi section based on biotic and sedimentary correlations), may indicate the boundary between the MFZs 14 and 15 (Poty et al., 2006). In addition, the association of the colonial rugose coral genera *Diphyphyllum* and *Siphonodendron* can be attributed to the rugose coral association 4 (RCA4) of the late Asbian to Brigantian age (MFZs 14 to 15) (Somerville and Rodríguez, 2007). Hence, the small coral and coral-microbial-bryozoan reefs in the lower part (28.55 m to 30.5 m and 31 m to 38.5 m) and the large coral reef in the upper part (76 m to 92 m) of the Gandongzi section are of late Asbian (MFZ 14, RC7β) and early Brigantian (MFZ 15, lower RC8) age, respectively.

The coral reef from the Xiadong section is also found in the Du'an Formation. Abundant typical late Visean foraminifer taxa occur in the reef and its underlying and overlying beds, including *Bradyina* cf. *rotula*, *B.* sp., *Climacammina* sp., *Cribrostomum* sp., *Endothyra* sp., *Endothyranopsis* ex gr. *hirosei*, *E.* sp., *Eostaffella* cf. *acutiformis*, *E. postmosquensis*, *E.* sp., *Palaeotextularia* sp., *Plectostaffella* ex gr. *bogdavokensis*, *P.* sp., *Pseudoendothyra* sp., and *Tetrataxis* sp. The occurrence of *Climacammina* sp. suggests a latest Visean (MFZ 15) age (Poty et al., 2006). The reef consists of abundant colonial rugose coral species belonging to *Diphyphyllum*, *Lithostrotion* and *Siphonodendron*, suggesting they probably belong to RCA 4 of the late Asbian to early Brigantian (MFZs 14 to 15) (Somerville and Rodríguez, 2007; Denayer, 2014). In addition, the Xiadong coral reef contains a rugose coral assemblage similar to the nearby upper coral reef at

Gandongzi, implying that both are early Brigantian in age. Combining the foraminiferal and coral evidence, the age of the Xiadong reef is ascribed to the early Brigantian (lower MFZ 15). However, in South China, the precise comparison between the Mississippian foraminiferal and coral zonation needs further studies.

In the Yashui section, the foraminiferal biostratigraphy has been well studied, thus the Visean-Serpukhovian boundary was placed at 49 m height above the section base according to the first appearance of "tortula-like" specimens (Groves et al., 2012). The coral biostromes are developed in late Visean strata between 28 m and 32 m height above section base. Abundant and diverse foraminifers are present in the biostromes and their underlying and overlying strata, including *Archaediscus angulatus*, *Biseriella endothyra*, *B. parva*, *Bradyina* sp., *Climacammina* sp., *Cribrospira mikhailovi*, *C. panderi*, *C.* cf. *perretae*, *C.* sp., *Cribrostomum* sp., *Endostaffella* cf. *fucoides*, *E.* sp., *Endothyra prisca*, *E.* sp., *Endothyranopsis compressa*, *E. crassa*, *E.* sp., *Eostaffella mosquensis*, *E.* sp., *Koskinotextularia* sp., *Omphalotis* sp., *Palaeotextularia* sp., *Pseudoendothyra struvei*, *P.* sp., *Tetrataxis* sp., and *Warnantella* sp. The occurrence of *Climacammina* sp., *Koskinotextularia* sp., and *Biseriella parva*, indicates that the biostromes belong to the early Brigantian (lower MFZ 15 of Poty et al., 2006).

4. Material and methods

In this study, late Visean reef materials of South China were first documented, including field outcrops, polished slabs and thin sections. Field photographs were taken using Canon EOS 5D and Canon PowerShot SX60 HS digital cameras. Polished slabs and thin sections were produced at NIGP, and were photographed with scanner EPSON DS-50000 and microscope Nikon SMZ645,

respectively. The other described materials of the Mississippian bioconstructions are from Drs. Markus Aretz and Le Yao, based on long-term studies.

A Late Devonian-Mississippian palaeoreef database was constructed in this study using the methods of Kiessling et al. (2000) and Yao et al. (2016a), based on our own new and published data (Yao et al., 2016a). The weighted abundance of the studied bioconstructions was calculated according to their size (width and thickness). Values of 1, 2, 3 and 4 were assigned to bioconstruction corresponding to width of <10 m, 10 to 100 m, 101 to 1000 m and >1000 m, and thickness of <10 m, 10 to 100 m, 101 to 500 m and >500 m, respectively (Table 1). Values of weighted abundance for bioconstruction = (Assumed width value + Assumed thickness value) × Bioconstruction number. Site number for bioconstructions represents the number of bioconstruction locations. Values of weighted abundance for reef builders = bioconstruction weighted abundance × proportion ratio of reef builders × biotic content proxies. The proportion ratio of reef builders is derived from field observation and published reef descriptions. Biotic content proxies are of 1 and 0.7 for reefs and biostromes, and reef mounds respectively, due to different reef types containing various proportions of total biotic volume (Table 1). The rugose coral diversity was calculated by counting genera and species numbers, which were compiled by Markus Aretz and Le Yao from the published literatures and their own data.

The absolute age of carbon and strontium isotopic data is calibrated according to the Geological Time Scale 2016 (Ogg et al, 2016). The trend line of strontium isotope uses LOESS regression, 0.2 smoothing with 2.5% and 97.5% bootstrapped errors. The trend line of carbon isotope uses a two-point mean curve. Latitudinal distribution of glacial deposits is based on the data of documented glacial ages and locations, and their palaeolatitudes from the Late Devonian to

Mississippian (Supplementary Table 1).

5. Results

5.1. Mississippian bioconstructions

5.1.1. Tournaisian Stage

During the Tournaisian, no skeletal bioconstructions have been documented to date, although potential skeletal bioconstructions might have developed during this time (Webb, 2002; Aretz and Chevalier, 2007; Yao et al., 2016a). Further studies need to be done to test this hypothesis. Whereas, microbial bioconstructions are common during this time (Lees and Miller, 1985, 1995; Yao et al., 2016a). After the disappearance of stromatoporoid reefs during the Hangenberg mass extinction, microbial carbonate proliferation occurred (Yao et al., 2016a). Commonly, the bioconstructions consist of a microbial framework (thrombolites), which includes low-abundance skeletal biota without frameworks, such as rugose and tabulate corals, bryozoans, crinoids and calcareous algae (Webb, 1998, 2005; Yao et al., 2016a). Stromatolites were rare during this time, and are only known from northwestern China and eastern Australia (Webb, 1998, 2005; Yao et al., 2019; Fig. 3A-B). In the late Tournaisian, the abundance of shallow-water microbial bioconstructions declined, and deep-water Waulsortian mud mounds became abundant mainly around the Laurussia continent (Lees and Miller, 1985, 1995; Yao et al., 2016a; Fig. 3C). In South China, Waulsortian-like mud mounds occurred during this time (Aretz et al., 2012; Fig. 3D), which contain abundant polymuds, stromatactoid cavities and various bioclasts (e.g., crinoids, sponge spicules, bryozoans, brachiopods and ostracods). These mounds differ from Waulsortian mounds because they lack fenestellid bryozoans and stromatactis structures (Lees and Miller, 1985,

1995).

5.1.2. Visean Stage

Western Palaeotethys Ocean

In western Palaeotethys Ocean, on the shelves of southern Laurussia (Western and Central Europe) and northern Gondwana (northwestern Africa to southern Turkey), skeletal biota did not contribute to reef frameworks until the early Visean (Adams, 1984). One example of this age is from Furness (England), where a rigid framework is constructed by tabulate corals together with calcimicrobes and foraminifers (Adams, 1984). These reefs initiate a type of metazoan-microbial consortium, which is characteristic of many Visean reefs, such as the small middle Visean microbial-bryozoan reefs in the Dinant–Namur Basin, Belgium (Aretz and Chevalier, 2007), and large late Visean microbial-sponge-bryozoan-coral reefs in Cracoe, England and the Jerada Massif, Morocco (Mundy, 1994; Aretz and Herbig, 2008; Waters et al., 2017; Figs. 1B-C, 4A). During the middle Visean, metazoan bioconstructions occurred, characterized by coral biostromes in Belgium (Aretz, 2002). Coral bioconstructions became more common during the late Visean, including a few coral reefs from Wales (Aretz and Herbig, 2003a; Fig. 4B-C), southern France (Aretz and Herbig, 2003b) and Morocco (Aretz and Herbig, 2008; Aretz, 2010a; Rodríguez et al., 2012). They were mainly constructed by closely spaced, substrate-attached massive and branching colonial rugose corals (Fig. 4C). Much more common are coral biostromes in the Variscan realm (Rodriguez et al., 1994; Aretz & Chevalier, 2007; Aretz et al., 2010; Figs. 1C, 4D). They range from accumulation of coral debris (allobiostromes) to structures dominated by *in situ* coral framework (autobiostromes) (Fig. 4D). A few bryozoan reef mounds developed in Wales during

this time (Bancroft et al., 1988).

Western Panthalassa Ocean

In Queensland of Eastern Australia (eastern margin of Gondwana, southwestern Panthalassa Ocean), there is a continuous reef record throughout Visean times (Fig. 1A-C). Similar to the western Palaeotethys realm, metazoans began to form frameworks in the early Visean, represented by sponges and fasciculate rugose and tabulate corals together with microbes. This metazoan-microbial consortium persisted until the late Visean (Shen and Webb, 2005, 2008). Corals are more abundant in the reef frameworks and may even become volumetrically dominant during the late Visean (Webb, 1989, 1999; Fig. 4E). However, framework formation still relied on calcimicrobes (Shen and Webb, 2005, 2008). In Japan (western Panthalassa Ocean), abundant carbonates developed on the Akiyoshi and Kitakami seamounts, containing Mississippian skeletal bioconstructions. They were mainly constructed by colonial rugose corals, together with bryozoans, sponges, calcareous algae and calcimicrobes (Kawamura, 1989; Nakazawa, 2001; Figs. 1C, 4F). In northwestern China (eastern Tianshan orogenic belt, northwestern Panthalassa Ocean), the window for reef formation was only brief due to a position in higher latitudes. However, with more temperate conditions than most other regions of similar latitude, a few late Visean coral biostromes occur with thickness less than 5 m and width more than 1 km (Huang et al., 2019). Other reef types are not known from this region.

Eastern Panthalassa Ocean

Compared with western Palaeotethys and western Panthalassa oceans, Visean

bioconstructions are rare in eastern Panthalassic Ocean, especially for coral bioconstructions (Fig. 1B-C). During this time, only a few middle Visean sponge-microbial reef mounds developed in Alabama, USA (Kopaska-Merkel et al., 2013). To date, little is known about the contribution of corals to bioconstructions along the western margin of Laurussia continent.

Eastern Palaeotethys Ocean (South China)

Similar to western Panthalassa Ocean, Visean bioconstructions have been insufficiently studied in eastern Palaeotethys Ocean. A few coral biostromes have been reported from the middle Visean strata on the South China Block, which are mainly built by colonial and solitary rugose and tabulate corals (Yao et al., 2016b; Figs. 1B). Late Visean coral bioconstructions are documented here from South China (Figs. 1D and 5), including coral reefs, coral biostromes and coral frameworks. Three coral reefs are exposed in the Gandongzi and Xiadong sections, with thickness ranging from 2 m to 30 m and widths of up to 70 m (Fig. 5A-C). The reefs comprise *in situ* large rugose coral colonies of fasciculate growth form with width and height ranging from 1–2 m and 0.5–1 m, respectively (Fig. 5B-C). Colonies are closely spaced and substrate-attached, forming rigid frameworks with the interspaces filled with dwellers (e.g., crinoids and brachiopods), coral fragments and detrital carbonate sediments (Fig. 5C). Additionally, a tabulate coral framework with interconnected corals of fasciculate form was documented in a single, 8 m-thick coral-microbial-bryozoan reef at Gandongzi (Fig. 5D). Four coral biostromes are exposed in the Yashui section, which range in thickness from 0.2 m to 0.3 m and have a width of more than 10 m in outcrop. They consist primarily of fasciculate colonial corals, which are mainly in growth position (Fig. 5E). Coral reefs/frameworks differ from coral biostromes because of their abundant

microbial crusts and sparry calcite cement around coral skeletons, which consolidate the reef framework (Fig. 5F-M). Encrusting bryozoans and foraminifers further contributed to the rigid reef framework (Fig. 5N-O). Corals generally reproduced by asexual budding, assisting to form frameworks and cavities with dwellers developing habitat complexity (Fig. 5P). These coral bioconstructions were mainly constructed by species belonging to the colonial rugose coral genera *Diphyphyllum, Siphonodendron*, *Stylostrotion* and *Lithostrotion* and the tabulate coral genus *Syringopora* (Fig. 5H-L). Abundant associated fossils are present in the interspaces between the coral skeletons, including crinoids, brachiopods, foraminifers, bryozoans, gastropods, ostracods, and calcareous algae (Fig. 5G-L).

5.1.3. Serpukhovian Stage

Compared with the late Visean, the site number of skeletal bioconstructions declined in the Serpukhovian times (Fig. 1E-F), although corals remained the most common builders of skeletal bioconstructions (Figs. 1E-F, 6). A few coral reef mounds are reported from the Donets Basin, Ukraine in the late Serpukhovian (Ogar, 2012; Fig. 1F). More common are the coral biostromes developed in southern France (Aretz and Herbig, 2003a) and Alabama, USA (Kopaska-Merkel et al., 2013) in the early Serpukhovian and in northwestern China (Fig. 6A-B) and Béchar Basin, Algeria (Atif et al., 2016; Fig. 6C-D) during the late Serpukhovian (Fig. 1E-F). They are mainly built by fasciculate and massive colonial rugose corals (Fig. 6B, D). Metazoan-microbial bioconstructions were also present during this time, such as the chaetetid-coral-microbial reef in northwestern Georgia, USA (Lord et al., 2011), microbial-coral reef in southern France (Aretz and Herbig, 2003a, Cózar et al., 2019), and sponge-microbial-coral-bryozoan reef in Japan (Nakazawa,

2001; Fig. 1E-F). Rare microbial reefs occurred in the Serpukhovian, with a few examples described from the Timan-Ural area in Russia (Antoshkina, 1998) and may also be present in southern France (Cózar et al., 2019; Fig. 1E).

5.2. Late Devonian-Mississippian reef evolution

A high-resolution review of the age, abundance, composition and distribution of Late Devonian to late Mississippian skeleton- and microbe-dominated bioconstructions has been undertaken using a newly constructed global reef database (Supplementary Table 2). This confirms that abundant stromatoporoid-coral reefs declined in the late Frasnian, a trend that continued during F-F extinction before stromatoporoid reefs vanished entirely during the Hangenberg extinction (Fig. 7). Afterwards, no Tournaisian skeletal bioconstruction is known, although potential skeletal bioconstructors occurred during this time. Skeletal reefs reappeared in the early Visean, with a low abundance and restricted locations in the western Palaeotethys along the southeastern margin of Laurussia near the palaeoequator. Few metazoan frameworks are present in the microbial-metazoan reefs found at relatively high latitude along the northeastern margin of Gondwana in eastern Australia (Figs. 1A, 7). Their abundance slightly increased during the middle Visean, accompanied with extended distribution between the palaeoequator and 20° S (Figs. 1B, 7). However, reef ecosystems were still dominated by microbes at this stage, whereas bryozoan–coral constructions rarely occurred (Figs. 1A-B, 7). In late Visean times, skeletal reefs obviously increase in both abundance and latitudinal distribution, as they developed up to 40° both north and south of the palaeoequator (Figs. 1C, 7). They were mostly constructed by corals, with lesser contributions from bryozoans, sponges and calcareous algae (Figs. 1C, 7).

Microbe-dominated reefs also occurred in Western Europe and North Africa between the palaeoequator and 30° S at this time (Fig. 1C).

The precise timing of this coral reef recovery is seen within the Asbian to Brigantian substages (Figs. 7, 8). Early Asbian skeletal reefs are rare with a mixed composition of skeletal and microbial constituents (Fig. 8A). Corals began to replace bryozoans and they become the dominant metazoan constructors during this time (Fig. 8B). This was followed by a dramatic increase in abundance of skeletal (mainly coral) reefs during the late Asbian and a slight decrease in abundance but still with high value in the early Brigantian (Figs. 7, 8). Thus, there was a global coral-reef ecosystem acme during the late Asbian-early Brigantian interval. During late Brigantian times, coral reefs became rarer and reef ecosystems returned to the metazoan-microbial mixed type. The abundance of the skeletal reefs continued to decrease until the late Serpukhovian (Fig. 7), when reef distribution was contracted to the region between the palaeoequator and 30° S (Fig. 1E-F). However, corals remained the dominant component among the metazoan reef builders during this coral reef decline (Fig. 8B).

5.3. Mississippian biodiversity changes

Based on the high-resolution rugose coral data from Western Europe, the newly compiled species and genus diversity of the Mississippian rugose corals shows their close relationships with temporal patterns in coeval coral reefs (Fig. 9). Their diversity was continuously low from the early Tournaisian to early part of the late Visean (early Asbian), with a slight diversity increase during the late Tournaisian (Fig. 9). Then, during the middle part of the late Visean (late Asbian to early Brigantian), a prominent increase in the rugose coral diversity occurs both for species and

genus levels, followed by a dramatic diversity decline during the latest Visean (late Brigantian). This decreasing trend continues to the late Serpukhovian (Fig. 9).

A compilation of genus and species diversity was also conducted for key Mississippian metazoans including nektonic fauna (e.g., ammonoids) and benthic fauna (e.g., foraminifers and brachiopods) (Raymond et al., 1990; Korn and Ilg, 2008; Groves and Wang, 2009; Qiao and Shen, 2015), which provide insights into the correlations between coral reef ecosystem and biodiversity in the remainder of the marine ecosystem during this time. Similar to the variation curve in rugose coral diversity, low values of species and genus diversity are also present in ammonoids, foraminifers and brachiopods from the early Tournaisian to early part of the late Visean, although transient biodiversity increases occurred in the late Tournaisian (Fig. 9). During the middle part of the late Visean, a prominent diversity increase occurs both for nektonic and benthic faunas, which shows an overall slight decline until the late Serpukhovian (Fig. 9).

Accompanied with the diversity increase in nektonic and benthic faunas during the middle part of the late Visean, their composition also obviously changed. The diversity increase in the middle part of the late Visean rugose corals is represented by the occurrence of abundant new species belonging to the solitary coral genus *Axophyllum* and colonial coral genera *Diphyphyllum*, *Lithostrotion* and *Siphonodendron*, which are the main coral reef builders during this time (e.g., Aretz and Herbig, 2003b; Rodriguez et al., 2016; Fig. 5H-K). From the early Tournaisian to the early part of the late Visean, ammonoids are characterized by the superfamily of Dimorphocerataceae and family of Pericyclidae. Then, the distinct diversity increase in the middle part of the late Visean results from the appearance of new genera and species belonging to the superfamilies Medlicottiaceae and Neoglyphiocerataceae in the *Hypergoniatites-Ferganoceras*

genus zone (Korn and Ilg, 2008). In late Visean times, foraminifer diversity increased to 228 species with diversification of the superfamily Endothyroidea, including endothyroids, tetrataxids, palaeotextulariids and archaediscids (Groves and Wang, 2009). During the middle-late Mississippian, *Gigantoproductus* became a dominant component of brachiopod faunas, with 57 species known (Qiao and Shen, 2015). Diversity increased notably in the late Visean (MFZ 14), when brachiopod faunas are characterized by *G. edelbergensis* and *G. giganteus* (Qiao and Shen, 2015). Crinoid diversity also shows an increase at this time, with advanced cladids replacing camerate crinoids (Ausich and Kammer, 2013).

5.4. Mississippian palaeoenvironmental changes

The Mississippian is an important transitional interval from Devonian greenhouse to Permo-Carboniferous icehouse climates, accompanied with prominent tectonic activity (e.g., Gondwana and Laurussia continental collision) and plant evolution (Algeo and Scheckler, 1998; Nance and Linnemann, 2008; Montañez et al., 2011). Consequent changes in terrestrial weathering, climate (e.g., cooling or warming) and ocean chemistry (e.g., redox conditions), are recorded in sedimentary successions and geochemical proxies (Mii et al., 1999; Fielding et al., 2008; Grossman et al., 2008; Isbell et al., 2012; Yao et al., 2015; Maharjan et al., 2018a, b). In this study, inorganic carbon and strontium isotopes, glacial distribution and adjusted sea surface temperature (SST) were compiled for the early Frasnian (Late Devonian) to late Serpukhovian (Mississippian) interval, in order to assess climatic and oceanic changes (Fig. 10).

5.4.1. Marine anoxia

During the Earth history, one of the most important oceanic perturbations took place in the early Mississippian (middle part of Tournaisian, synonymous to mid-Tournaisian). During that time, anoxic conditions are widespread in basinal and slope settings, resulting in the deposition of black shales and/or dark siliceous deposits (e.g., Siegmund et al., 2002). In the shallow water, carbonate production slowed down or ceased, and black-greyish shales, marls and marly limestones were deposited, which indicate dysoxic to occasionally anoxic conditions (e.g., Poty et al., 2002, 2011; Yao et al., 2015).

This marine anoxia is also evidenced by isotopic records (e.g., Yao et al., 2015; Aretz, 2016; Maharjan et al., 2018b). A major, positive shift in inorganic carbon isotope occurred in the mid-Tournaisian, named as the "Tournaisian Carbon Isotope Excursion" (TICE; Yao et al., 2015; Fig. 10), and is seen in North America, Western Europe and South China (Mii et al. 1999; Saltzman et al., 2000, 2004; Yao et al., 2015; Maharjan et al., 2018a; Fig. 10). It has been related to the enhanced organic matter burial rates, resulting from widespread anoxic conditions (Mii et al, 1999). This hypothesis is supported by consistent variation in inorganic and organic carbon isotopes, indicating changes in ocean dissolved inorganic carbon due to organic matter burial (Maharjan et al., 2018a). Recent studies documented positive excursions in nitrogen and sulphur isotopes in South China and North America, suggesting enhanced water-column denitrification and sulphate reduction respectively, under increased organic carbon burial and expansion of oxygen minimum zone (Yao et al., 2015; Maharjan et al., 2018a, b). In addition, mid-late Tournaisian black shales developed on shallow platforms and slopes in South China and southern Laurussia (Yao et al., 2015; Aretz, 2016), which further supports the notion of increased organic burial rates at this time. Enhanced organic burial could have resulted in atmospheric CO_2

drawdown and climate cooling (Mii et al., 1999; Yao et al., 2015), consistent with positive oxygen isotopic excursion during the TICE interval (Mii et al., 1999; Buggisch et al., 2008; Grossman et al., 2008; Fig. 10).

5.4.2. Glacial-interglacial alternation

Glacial-interglacial alternations in the Mississippian are evidenced from recurrent glacial deposits widely developed on the Gondwana continent at high latitudes (Fielding et al., 2008; Isbell et al., 2012). The oldest occur in the Late Devonian (middle Famennian Stage) of South America (Brazil, Bolivia and Peru) (Isaacson et al., 2008). Their distribution expanded into South America and Africa (Central African Republic, Niger) and North America (eastern USA) to the lowest latitude of about 40° S during the latest Devonian (Strunian) (Brezinski et al., 2008; Isaacson et al., 2008; Fig. 10). In succeeding Mississippian times, glacial-interglacial alternations continuously developed, as glaciations waxed and waned on the Gondwana continent (Fig. 10). The first Mississippian glacial climate is in the mid-Tournaisian, with glacial deposits in South America (Argentina and Brazil) consistent with positive carbon and oxygen isotopic excursions during this time (Buggisch et al., 2008; Caputo et al., 2008; Césari et al., 2011; Fig. 10). Then, glaciation was intermittently developed in the late Tournaisian, early Visean and early part of the late Visean, in South America (Argentina, Bolivia, Brazil and Patagonia) and Africa (South Africa). The lowest latitude of glacial deposits occurred between 40° S and 65° S (Caputo et al., 2008; Césari et al., 2011; Isbell et al., 2012; Limarino et al., 2014; Fig. 10). During the Serpukhovian, glacial deposition greatly expanded and became widely distributed in South America (Argentina and Brazil) and Australia (Fielding et al., 2008; Césari et al., 2011; Limarino et al., 2014). The

lowest glacial latitude may reach to 25° S in eastern Australia, indicating that the main phase of the Permo-Carboniferous icehouse climate occurred during this time (Fig. 10).

The Mississippian glacial-interglacial alternations are manifest in low-middle latitude areas, indicated by relative sea-level fluctuations with sedimentary facies changes (Poty, 2016; Yao and Wang, 2016; Yao et al., 2016c). On the South China Block located near the palaeoequator in eastern Palaeotethys Ocean, frequent regressive episodes were accompanied with non-carbonate, dolostone facies and hiatuses in the mid-Tournaisian, early Visean and Serpukhovian, which are consistent with the coeval glaciation on the Gondwana continent (Yao and Wang, 2016). In the Namur-Dinant Basin (southern Belgium) near the palaeoequator in western Palaeotethys Ocean, frequent Mississippian sedimentary sequences were discerned, which were related to glacial climate during this time (Poty, 2016). During the Tournaisian, third-order sequences recorded large sea-level variations, which are considered to be due to glacioeustasy. At the Tournaisian-Visean boundary, the strong sea-level fall may represent the onset of the obvious Permo-Carboniferous glaciations. During the Visean, eccentricity cycles developed, recording frequent interglacial-glacial alternations (Poty, 2016). During the Mississippian, ice caps widely developed on the Gondwana (South Polar region), resembling modern times, could have caused a hurricane zone at middle latitudes between 10° to 30°. Hence, the brachiopod storm shell beds widely occurring in the South China Block and North Africa from the latest Visean to Serpukhovian, also indirectly support the notion of glaciation at this time (Rodríguez et al., 2016; Yao et al., 2016c). In addition, the glacial-interglacial alternations correspond to contemporaneous changes in sea-surface temperature calculated from oxygen isotope data (Ogg et al., 2016; Fig. 10).

5.4.3. Late Visean warm climate

Multiple lines of evidence suggest that a warm climate occurred during the late Visean, including sedimentary, biotic and isotopic records (Iannuzzi and Pfefferkorn, 2002; Giles, 2012; Isbell et al., 2012; Qiao and Shen, 2015). For example, no glacial deposits are known from the middle part of the late Visean (MFZ14-15) (Caputo et al., 2008; Isbell et al., 2012; Limarino et al., 2014; Fig. 10). Following the prominent glacioeustatic changes at the Tournaisian-Visean boundary, another main phase of glacioeustatic-style sea-level change occurs around the Visean-Serpukhovian transition (middle Brigantian to early Serpukhovian) in the United States, South China and England, which coincide with Gondwanan glacial deposits (Smith and Read, 2000; Fielding and Frank, 2015; Chen et al., 2016, 2019). In addition, late Visean warm climate is also indicated by the width and extent of the Paraca floral belt in the southern hemisphere (Peru, Bolivia, Brazil, Niger, India and Australia) between 30° S and 60° S (Iannuzzi and Pfefferkorn, 2002). The flourishing of gigantoproductid fauna during the late Visean (MFZ14-15) is also attributed to climate warming, with their diversity decrease blamed on Gondwanan glaciation in the following Serpukhovian (Qiao and Shen, 2015; Fig. 9). Changes in sea-water temperature during the late Visean are also manifest in oxygen isotope and trace element records (Armendáriz et al., 2008; Powell et al., 2009; Giles, 2012). Based on brachiopod oxygen isotope, the high point of the Carboniferous warm period occurred in the late Visean (late Asbian to Brigantian) (Giles, 2012). Tropical sea-water temperature is suggested to have reached ~20 °C on average with a mean range from ∼10 °C to ∼33 °C during this time, according to the analysis of brachiopod trace elements (Powell et al., 2009). This was followed by cooling, inferred from oxygen isotope data in the late Brigantian (Armendáriz et al., 2008). The late Visean warm period coincides with the low

values of inorganic carbon and strontium isotopic ratios. This is followed by a positive shift in strontium isotope ratios, resulting from enhanced continental weathering rates that leads to glacial climate (Saltzman and Thomas, 2012; Chen et al., 2018; Fig. 10).

6. Discussion

6.1. Delayed re-emergence of Mississippian coral reef ecosystems

After the disappearance of skeletal reefs during the Hangenberg extinction, the succeeding Mississippian has long been known as an interval dominated by microbial reefs, especially the Waulsortian mud mounds (Heckel, 1974; Lees and Miller, 1985). Afterwards, skeletal reefs were gradually found and systematically reviewed during the middle-late Mississippian, suggesting a metazoan recovery phase occurs during this time, but without a single, dominant reef community (e.g. Webb, 1994, 2002). Recently, more skeletal reefs were reported from the Visean Stage (Aretz and Chevalier, 2007; Yao and Wang, 2016), especially coral bioconstructions (Aretz and Herbig, 2003a, b; Aretz et al., 2010; Ogar, 2012; Rodríguez et al., 2012; Yao et al., 2016b; Huang et al., 2019). Reports of late Visean coral bioconstructions in western Palaeotethys and Panthalassa oceans mark the first appearance of metazoan reef proliferation since the Hangenberg extinction (e.g., Aretz and Herbig, 2003a, b; Rodríguez et al., 2012; Figs. 1, 4). In this study, the documentation of coeval coral bioconstructions from the South China Block, further suggests that this recovery may have been a widespread phenomenon (Figs. 1d, 5). Our newly constructed global, high-resolution reef database, confirms this hypothesis and shows that both abundance and distribution of coral reefs reached an acme from the late Asbian to early Brigantian (Figs. 1, 7, 8). Even compared with microbial bioconstructions, the late Asbian-early Brigantian coral

bioconstruction abundance is higher, indicating that coral reef ecosystems proliferated and became the dominant component in the marine ecosystem during this time (Fig. 8A).

Although metazoan reefs proliferated in the Phanerozoic, reef crises and recoveries commonly occurred during mass extinction transitions (Kiessling et al., 1999; Flügel and Kiessling, 2002). The duration of metazoan reef-recovery intervals varies considerably, probably because of the varying intensity of extinctions and palaeoenvironmental conditions afterwards (Flügel and Kiessling, 2002; Lee et al., 2015; Yao et al., 2016a). According to the classification of Flügel and Kiessling (2002), three sub-intervals could be discerned during metazoan reef-recovery: (1) metazoan "reef gap" phase, (2) metazoan reef re-establishment phase, and (3) metazoan reef proliferation phase (Fig. 7). During the Phanerozoic, in addition to the Mississippian, the other two notable metazoan reef-recovery intervals are the middle-late Cambrian and Early Triassic (Lee et al., 2015; Martindale et al., 2018; Fig. 11). For example, metazoan "reef gap" delays of about 5 Ma and 2 Ma respectively are reported after the extinction of archaeocyath and sponge-coral-algae reef ecosystems at the early-middle Cambrian and Permian-Triassic extinction transitions. Sponge and sponge-bivalve-coral reefs reappeared during the Drumian Stage and Olenekian Stage (Smithian Substage), respectively (Brayard et al., 2011; Adachi et al., 2015; Fig. 11). However, for these examples, true metazoan reef proliferation only occurred much later, in the late Cambrian (Jiangshanian Stage) and Middle Triassic (late Anisian Stage) about 15 Ma and 9 Ma after their respective mass extinctions (Lee et al., 2015; Martindale et al., 2018; Fig. 11). In contrast, in the Mississippian, the metazoan "reef gap" lasted for more than 12 Ma (the whole Tournaisian Stage) and the recovered global coral reef ecosystems did not appear until the late Visean (late Asbian Substage) for about 23 Ma after the Hangenberg crisis (Fig. 11). Hence,

compared with the notable metazoan reef-recovery intervals during the middle-late Cambrian and Early-Middle Triassic, proliferation of the Mississippian coral reef ecosystems was the most prolonged of the Phanerozoic.

6.2. Coupled trend between skeletal reef and biodiversity

During the Phanerozoic, a positive correlative relationship occurred between reef genera and the total recorded genera, which suggests that reefs are sources of marine biodiversity (Kiessling et al., 2010). This is also supported by the positive correlation between diversity variation trend of skeletal reef builders with that of the total biodiversity (Wood, 1999). In addition, the increase in abundance of skeletal bioconstructions is consistent with the decrease in abundance of microbial bioconstructions, which implies that the diversity changes in skeletal bioconstructors are the main controlling factor on microbial development, especially through mass extinction transitions (Yao et al., 2016a). These all indicate that skeletal reefs are important components of marine ecosystems, and have a close relationship to total marine biodiversity. To test this idea, we have compared the abundance of Mississippian skeletal reefs with coeval marine biodiversity (Fig. 9). From the early Tournaisian to early part of the late Visean, the abundance of skeletal reefs remains low, except for a slight increase during the middle Visean. This low reef abundance closely corresponds to the low diversity for both nektonic and benthic faunas during this time, except for a transient decoupled trend in the late Tournaisian when relative biodiversity increases (Fig. 9). Coinciding with the obvious increase in the abundance of skeletal reefs (mainly coral reefs), the diversity of nektonic and benthic faunas greatly increased in the middle part of the late Visean, especially for rugose corals which attained a peak value (Fig. 9). Then, skeletal reefs decreased in

abundance until the late Serpukhovian, which coincides with diversity decline of rugose corals and brachiopods and slight decreases in ammonoid and foraminifer diversity (Fig. 9). Thus, the evolution of metazoan reefs follows overall biodiversity trends amongst marine taxa. During the late Visean, the re-establishment of complex structures and niches in the coral reef ecosystems is an important factor in the increase of marine biodiversity, implying that the conditions that allowed metazoan reef recovery are also beneficial to all marine ecosystems.

6.3. Controlling factors

Reefs as aquatic biosedimentary structures represent complex marine ecosystems formed by benthic communities, which created and maintain topographic relief through the formation of carbonate deposition (Riding, 2002). Hence, their growth and demise are closely related to biotic evolution and palaeoenvironmental changes (Wood, 1999; Aretz and Chevalier, 2007; Kiessling, 2009; Yao and Wang, 2016). During the Mississippian, coral reef abundance shows a more positive correlation with genus and species diversity of colonial rugose corals, which are the main reef builders, than with the total diversity of rugose corals (Figs. 9, 12). The diversity of colonial rugose corals was low until the middle part of the late Visean when a dramatic increase in diversity occurred accompanied with coral reef proliferation. The subsequent diversity decrease coincided with the decrease coral reef abundance (Fig. 12). Hence, the evolutionary pattern of Mississippian coral reefs is coupled with the diversity changes in colonial rugose corals, implying that reef-builder flourishment results in reef proliferation (Fig. 12).

After the Hangenberg extinction, crinoids quickly radiated and their diversity reached a maximum value of the Phanerozoic with the deposition of abundant crinoidal limestones during

the late Tournaisian (Ausich and Kammer, 2013; Debout and Denayer, 2018). Debout and Denayer (2018) showed that these crinoidal limestones contain an impoverished fauna of solitary rugose corals compared to other late Tournaisian shallow-water limestones. Hence, the success of crinoids may have indirectly influenced the development of skeletal reefs by negatively impacting coral diversity and/or abundance, which as shown above forms an important reservoir for bioconstructors. However, more detailed studies are required to uncover this potential link.

Palaeoenvironmental factors of different time scales could cause different-level changes in reef ecosystems. The long-term (million to tens of million years) palaeoenvironmental changes could lead to the changes in the composition and evolutionary pattern of reef ecosystems (Wood, 1999). In the middle-late Cambrian and Early Triassic, delayed metazoan reef recovery has been linked to persistent and severe environmental conditions, particularly the development of widespread ocean anoxia at these times (Wignall and Twitchett, 2002; Lee et al., 2015). Similar to the middle-late Cambrian and Early Triassic, harsh oceanic conditions were also present during the Mississippian, which could have hindered the metazoan reef recovery during this time (Figs. 10, 12). Widespread anoxia occurred during the mid-Tournaisian, evidenced by the paired positive shifts in carbon and sulfur isotopes and black shale deposits (e.g. Lower Alum Shale Event in southern Laurussia continent) during this time (Aretz, 2016; Maharjana et al., 2018b; Fig. 10). Enhanced organic burial could be responsible for atmospheric CO_2 drawdown and cooling that led to the development of Gondwanan glaciation in the mid-late Tournaisian (Mii et al., 1999; Isbell et al., 2012; Yao et al., 2015; Figs. 10, 12). Hence, marine anoxia with cooling climate during the mid-Tournaisian, may have delayed the recovery in marine ecosystems with no skeletal bioconstructions and low biodiversity during this time (Fig. 12). This hypothesis was supported by

the abundance and diversity of marine fauna remained low and almost unchanged during the mid-Tournaisian anoxia event (Fig. 9).

Beginning in the early Visean, marine environments gradually ameliorated and a warming trend may have favoured the appearance of metazoan reefs (Fig. 12). However, glaciations continuously developed during the early to early part of the late Visean, characterized by widely distributed glacial deposits on the Gondwana continent during this time (Caputo et al., 2008; Césari et al., 2011; Isbell et al., 2012; Limarino et al., 2014; Figs. 10, 12). These recurrent glacial climates accompanied with dramatic sea-level fall and non-carbonate facies development may have impeded metazoan reef proliferation (Fig. 12). The dramatic warming of climate during the middle part of the late Visean (MFZ14-15) resulted in the spread of warm, relatively well ventilated environments, which likely favoured coral-reef ecosystem resurgence and coral diversification. During the latest Visean to Serpukhovian, climate cooling was strengthened with expanded glacial development to lower latitudes, consistent with low sea-water temperature and positive strontium isotopic excursion (Isbell et al., 2012; Ogg et al., 2016; Chen et al., 2018; Figs. 10, 12). The widespread glacial development and intensified tectonic activity resulted in regional disappearance of carbonate shelves and extensive distribution of non-carbonate facies during the latest Visean to Serpukhovian, which cause the obvious decrease in skeletal reef abundance and decline of coral-reef ecosystems during this time (Fig. 12).

Photosymbiosis is an important factor in modern coral reef ecosystems: coral symbionts (e.g., zooxanthellae) enhance calcification and allow the construction of large colonies (Stanley, 2006; Stanley and Lipps, 2011). During the Phanerozoic, metazoan reef evolution was inferred to be closely related to photosymbiosis, with their proliferation and collapse consistent with the

occurrence and absence of photosymboints, respectively (Talent, 1988; Stanley and Lipps, 2011; Zapalski and Berkowski, 2019). According to detailed studies on morphologic comparisons (e.g., diameter and integrative level) and carbon and oxygen isotopes on Givetian-Frasnian and Famennian tabulate corals, it appears that the extinction of photosymbiotic bionconstructors probably caused the late Frasnian decline in stromatoporoid-coral reefs (Zapalski 2014; Zapalski et al. 2017a, b). Afterwards, the low abundance of Famennian metazoan reefs, was also related to the lack of photosymbionts during this time (Zapalski et al. 2017a, b).

However, the presence of photosymbionts has only been suggested for Devonian tabulate corals, and not for rugose corals which represent the bulk of the Mississippian corals in terms of abundance and diversity (Aretz, 2010b). The criteria of Coates and Jackson (1987) and Stanley and Lipps (2011) to identify possible photosymbionts, especially in colonial forms as potential bioconstructors, have not been successfully applied for Mississippian rugosa. On the other hand, the occurrence of photosymbiosis is not always accompanied with reef proliferation. In the Early Devonian, photosymbiotic bioconstructors (tabulate corals) were present, but the abundance of coral reefs was relatively low, which indicates that palaeoenvironmental changes (e.g. relative sea-level fall with siliciclastic facies development) primarily controlled on reef development during this time (Copper, 2002). Hence, the impact of photosymbiosis on the Late Palaeozoic reef evolution requires further detailed studies, but the current data do not indicate an influence of photosymbionts on the Mississippian reef recovery.

7. Conclusions

(1) The composition and distribution of the global Mississippian bioconstructions are described,

especially for coral bioconstructions. These show that coral reefs, coral frameworks and coral biostromes became widely developed in the late Visean times. This marks the first metazoan reef proliferation after the disappearance of stromatoporoid reefs during the end-Devonian Hangenberg extinction.

(2) Abundant coral reefs, coral frameworks and coral biostromes are documented in detail from the late Visean strata on the South China Block. They were mainly formed by the colonial rugose genera *Diphyphyllum, Siphonodendron*, *Stylostrotion* and *Lithostrotion* and the tabulate coral genus *Syringopora*. Coral reefs/frameworks differ from coral biostromes as their abundant microbial crusts and sparry calcite cement developed around coral skeletons, which consolidate the reef framework. These features are absent from the biostromes. Abundant associated fossils are present in the interspaces between the coral skeletons, including crinoids, brachiopods, foraminifers, bryozoans, gastropods, ostracods, and calcareous algae. The occurrence of the coral bioconstructions in South China (eastern Palaeotethys Ocean) further suggests that the late Visean coral reef recovery may have been a widespread phenomenon, mirroring their development in western Palaeotethys Ocean (Europe and North Africa).

(3) A high-resolution Late Devonian to late Mississippian reef database was constructed including the age, abundance, composition and distribution of skeleton- and microbe-dominated bioconstructions during this time. Based on this reef database, three sub-intervals of the Mississippian metazoan reef recovery were distinguished: 1) a metazoan “reef gap” phase without metazoan reefs during the Tournaisian; 2) a metazoan reef re-establishment phase consisting of a few metazoan reef occurrences from the early Visean to early part of the late Visean; and 3) a metazoan reef proliferation phase when coral reefs flourished over broad areas during the middle

part of the late Visean (late Asbian to early Brigantian substages). The re-establishment phase began at c. 347 Ma, about 12 Ma after the Hangenberg crisis (359 Ma), whilst it was 23 Ma (c. 336 Ma) before reefs proliferated; the longest post-extinction reef recovery delay of the Phanerozoic.

(4) Changes in the abundance of the Mississippian skeletal reefs are consistent with the diversity changes in marine nektonic and benthic faunas during this time, which indicated that skeletal reefs are the dominant constituents in marine environments and closely track overall marine biodiversity. Late Visean coral reef proliferation coincided with a global increased nektonic and benthic diversity.

(5) The exceptionally long delay for reef re-establishment in the Mississippian is suggested to be due to harsh oceanic conditions. During the mid-Tournaisian, anoxia was widespread. Whilst, intense but intermittent glaciations on the Gondwana suggest frequent cool episodes during the Mississippian. The development of a warm period in the late Visean (late Asbian to early Brigantian substages), finally favoured reef recovery.

Acknowledgements

We thank M.R. Saltzman of Ohio State University for providing the published carbon isotope data, Q.L Wang of Nanjing Institute of Geology and Palaeontology (NIGP) for preparing and discussing ammonoid biodiversity data, and J. Denayer of Liège University for providing field photo. The constructive reviews of J. Denayer and three anonymous reviewers greatly improved the manuscript. This work was supported by the Strategic Priority Research Program (B) of the Chinese Academy of Sciences (grant nos. XDB26000000, XDB18000000), the National Natural

Science Foundation of China (grant nos. 41902023, 41630101), and the Natural Science Foundation of Jiangsu Province (grant no. BK20181107).

References

Adachi, N., Kotani, A., Ezaki, Y., Liu, J., 2015. Cambrian Series 3 lithistid sponge-microbial reefs in Shandong Province, North China: reef development after the disappearance of archaeocyaths. Lethaia 48, 405–416.

Adams, A.E., 1984. Development of algal-foraminiferal-coral reefs in the Lower Carboniferous of Furness, northwest England. Lethaia 17, 233–249.

Algeo, T.J., Scheckler. S.E., 1998. Terrestrial marine teleconnections in the Devonian: links between the evolution of land plants, weathering processes, and marine anoxic events. Phil. Trans. Biol. Sci. 353, 113–130.

Antoshkina, A I., 1998. Organic buildups and reefs on the Palaeozoic carbonate platform margin, Pechora Urals, Russia. Sed. Geol. 118, 87–211.

Aretz, M., 2002. Habitatanalyse und Riffbildungspotential kolonialer rugoser Korallen im Unterkarbon (Mississippium) von Westeuropa. Köln. Forum Geol. Paläontol. 10, 1–155.

Aretz, M., Herbig, H.-G., 2003a. Coral-rich bioconstructions in the Viséan (Late Mississippian) of Southern Wales (Gower Peninsula, UK). Facies 49, 221–242.

Aretz, M., Herbig, H.-G., 2003b. Contribution of rugose corals to Late Viséan and Serphukovian bioconstructions in the Montagne Noire (Southern France). In: Ahr, W.M., Harris, P.M., Morgan, W.A., Somerville, I.D. (Ed.), Permo-Carboniferous Carbonate Platforms and Reefs. SEPM Mem. Spec. Pub. 78, 119–132.

Aretz, M., Chevalier, E., 2007. After the collapse of stromatoporid-coral reefs—the Famennian and Dinantian reefs of Belgium: much more than Waulsortian mounds. s. In: Álvaro, J.J., Aretz, M., Boulvain, F., Munnecke, A., Vachard, D., Vennin, E. (Ed.), Palaeozoic Reefs and

Bioaccumulations: Climatic and Evolutionary Controls. Geo. Soc. London Spec. Pub. 275, 163–188.

Aretz, M., Herbig, H.-G., 2008. Microbial-sponge and microbial metazoan buildups in the Late Viséan basin-fill sequence of the Jerada Massif (Carboniferous, NE Morocco). Geol. J. 43, 307–336.

Aretz, M., 2010a. Rugose corals from the upper Viséan (Carboniferous) of the Jerada Massif (NE Morocco): taxonomy, biostratigraphy, facies and palaeobiogeography. Paläontol. Z. 84, 323-344.

Aretz, M., 2010b. Habitats of colonial rugose corals: the Mississippian of western Europe as example for a general classification. Lethaia 43, 558-572.

Aretz, M., Herbig, H.-G., Somerville, I.D., Cózar, P., 2010. Rugose coral biostromes in the late Viséan (Mississippian) of NW Ireland: bioevents on an extensive carbonate platform. Palaeogeogr. Palaeoclimatol. Palaeoecol. 292, 488–506.

Aretz, M., Poty, E., Devuyst, F.-X., Hance, L., Hou, H., 2012. Late Tournaisian Waulsortian-like carbonate mud banks from South China (Longdianshan Hill, central Guangxi): preliminary investigations. Geol. J. 47, 450–461.

Aretz, M., 2016. The Kulm Facies of the Montagne Noire (Mississippian, southern France). Geol. Belg. 19, 69–80.

Armendáriz, M., Rosales, I., Quesada, C., 2008. Oxygen isotope and Mg/Ca composition of Late Viséan (Mississippian) brachiopod shells from SW Iberia: Palaeoclimatic and palaeogeographic implications in northern Gondwana. Palaeogeogr. Palaeoclimatol. Palaeoecol. 268, 65–79.

Atif, K.F.T., Aretz, M., Legrand-Blain, M., Bouzid, A., Aimouche, M., 2016. Brachiopods and rugose corals in an upper Serpukhovian (Mississippian) biostrome: preliminary results from the Djebel Arhlal (Béchar Basin, Algeria). Bol. Geol. Min. 127, 345–360.

Ausich, W.I., Kammer, T.W., 2013. Mississippian crinoid biodiversity, biogeography and macroevolution. Palaeontology 56, 727–740.

Bancroft, A.J., Somerville, I.D., Strank, A.E., 1988. A bryozoan buildup from the Lower Carboniferous of North Wales. Lethaia 21, 1–65.

Blakey, R., 2011. Global Paleogeography. http://jan.ucc.nau.edu/~rcb7/globaltext2.html.

Brayard, A., Vennin, E., Olivier, N., Bylund, K.G., Jenks, J., Stephen, D.A., Bucher, H., Hofmann, R., Goudemand, N., Escarguel, G., 2011. Transient metazoan reefs in the aftermath of the end-Permian mass extinction. Nat. Geosci. 4, 693–697.

Brezinski, D.K., Cecil, C.B., Skema, V.W., Stamms, R., 2008. Late Devonian glacial deposits from the eastern United States signal an end of the mid-Paleozoic warm period. Palaeogeog. Palaeoclimat. Palaeoecol. 268, 143-151.

Bruckschen, P., Bruhn, F., Veizer, J., Buhl, D., 1995. $^{87}Sr/^{86}Sr$ isotopic evolution of Lower Carboniferous seawater: Dinantian of western Europe. Sediment. Geol. 100, 63–81.

Bruckschen, P., Oesmann, S., Veizer, J., 1999. Isotope stratigraphy of the European Carboniferous: proxy signals for ocean chemistry, climate, and tectonics. Chem. Geol. 161, 127–163.

Buggisch, W., Joachimski, M.M., Sevastopulo, G., Morrow, J.R., 2008. Mississippian $\delta^{13}Cc_{arb}$ and conodont apatite $\delta^{18}O$ records – their relation to the Late Palaeozoic Glaciation. Palaeogeogr. Palaeoclimatol. Palaeoecol. 268, 273–292.

Caputo, M.V., Melo, J.H.G., Streel, M., Isbell, J.L., 2008. Late Devonian and Early Carboniferous

glacial records of South America. In: Fielding, C.R., Frank, T.D., Isbell, J.L. (Ed.), Resolving the Late Paleozoic Ice Age in Time and Space. Geol. Soc. Am. Spec. Paper 441, 161–173.

Césari, S., Limarino, C., Gulbranson, E., 2011. An Upper Paleozoic bio-chronostratigraphic scheme for the western margin of Gondwana. Earth Sci. Rev. 106, 149–160.

Chen, Z.Q., Benton, M.J., 2012. The timing and pattern of biotic recovery following the end-Permian mass extinction. Nat. Geosci. 5, 375–383.

Chen, J.T., Montañez, I.P., Qi, Y.P., Wang, X.D., Wang, Q.L., Lin, W., 2016. Coupled sedimentary and $\delta^{13}C$ records of late Mississippian platform-to-slope successions from South China: insight into $\delta^{13}C$ chemostratigraphy. Palaeogeogr. Palaeoclimatol. Palaeoecol. 448, 162–178.

Chen, J.T., Montañez, I.P., Qi, Y.P., Shen, S.Z., Wang, X.D., 2018. Strontium and carbon isotopic evidence for decoupling of pCO_2 from continental weathering at the apex of the late Paleozoic glaciation. Geology 46, 395–398.

Chen, J.T., Sheng, Q.Y., Hu, K.Y., Yao, L., Lin, W., Montañez, I.P., Tian, X.X., Qi, Y.P., Wang, X.D., 2019. Late Mississippian glacio-eustasy recorded in the eastern Paleo-Tethys Ocean (South China). Palaeogeogr. Palaeoclimatol. Palaeoecol. 531, 108873.

Copper, P., 1994. Ancient reef ecosystem expansion and collapse. Coral Reefs 13, 3–11.

Copper, P., 2002. Silurian and Devonian reefs: 80 Myr of global greenhouse between two ice ages. In: Kiessling, W., Flügel, E., Golonka, J. (Ed.), Phanerozoic reef patterns. SEPM Spec. Publ. 72, 181–238.

Copper, P., Scotese, C.R., 2003. Megareefs in Middle Devonian supergreenhouse climates. Geol. Soc. Am. Spec. Pap. 370, 209–230.

Copper, P., 2011. 100 million years of reef prosperity and collapse: Ordovician-Devonian.

Paleontol. Soc. Spec. Pap. 17, 15–32.

Coates, A.G., Jackson, J.B.C., 1987. Clonal growth, algal symbiosis, and reef formation by corals. Paleobiology 13, 363–378.

Cózar, P., Izart, A., Somerville, I.D., Aretz, M., Coronado, I., Vachard, D., 2019. Environmental controls on the development of Mississippian microbial carbonate mounds and platform limestones in southern Montagne Noire (France). Sedimentology 66, 2392–2424.

Denayer, J., 2014. Viséan Lithostrotionidae (Rugosa) from Zonguldak and Bartin (NW Turkey). B Geosci. 89, 737–771.

Debout, L., Denayer, J., 2018. Palaeoecology of the Upper Tournaisian (Mississippian) crinoidal limestones from South Belgium. Geol. Belg. 21, 111–127.

Domeier, M., Torsvik, T.H., 2014. Plate tectonics in the late Paleozoic. Geosci. Front. 5, 303-350.

Feng, Z.Z., Yang, Y.Q., Bao, Z.D., 1998. Lithofacies paleogeography of the Carboniferous in South China. J. Palaeogeogr. 1, 75–86.

Fielding, C.R., Frank, T.D., Isbell, J.L., 2008. The late Paleozoic ice age—a review of current understanding and synthesis of global climate patterns. In: Fielding, C.R., Frank, T.D., Isbell, J.L. (Ed.), Resolving the Late Paleozoic Ice Age in Time and Space. Geol. Soc. Am. Spec. Paper 441, 343–354.

Fielding, C.R., Frank, T.D., 2015. Onset of the glacioeustatic signal recording late Palaeozoic Gondwanan ice growth: New data from palaeotropical East Fife, Scotland. Palaeogeogr. Palaeoclimatol. Palaeoecol. 426, 121–138.

Flügel, E., Kiessling, W., 2002. Patterns of Phanerozoic reef crises. In: Kiessling, W., Flügel, E., Golonka, J. (Ed.), Phanerozoic reef patterns. SEPM Spec. Publ. 72, 691–733.

Flügel, E., 2004. Microfacies of carbonate rocks. Springer-Verlag Press, pp. 1–976.

Giles, P.S., 2012. Low-latitude Ordovician to Triassic brachiopod habitat temperatures (BHTs) determined from $\delta^{18}O_{[brachiopod\ calcite]}$: A cold hard look at ice-house tropical oceans. Palaeogeogr. Palaeoclimatol. Palaeoecol. 317-318, 134–152.

Grossman, E.L., Yancey, T.E., Jones, T.E., Bruckschen, P., Chuvashov, B., Mazzullo, S.J., Mii, H.S., 2008. Glaciation, aridification, and carbon sequestration in the Permo-Carboniferous: the isotopic record from low latitudes. Palaeogeogr. Palaeoclimatol. Palaeoecol. 268, 222–233.

Groves, J.R., Wang, Y., 2009. Foraminiferal diversification during the late Paleozoic ice age. Paleobiology 35, 367–392.

Groves, J.R., Wang, Y., Qi, Y.P., Richards, B.C., Ueno, K., Wang, X.D., 2012. Foraminiferal biostratigraphy of the Viséan-Serpukhovian (Mississippian) boundary interval at slope and platform sections in southern Guizhou (South China). J. Paleontol. 86, 753–774.

Hallam, A., Wignall, P.B., 1997. Mass Extinctions and Their Aftermath. Oxford University Press, Oxford, pp. 1–320.

Hance, L., Hou, H.F., Vachard, D., 2011. Upper Famennian to Visean Foraminifers and some carbonate Microproblematica from South China—Hunan, Guangxi and Guizhou. Geological Publishing House, Beijing, pp. 1–359.

Heckel, P.H., 1974. Carbonate buildups in the geologic record: a review. In: Laporte, L.F. (Ed.), Reefs in Time and Space. SEPM Spec. Publ. 18, 90–154.

Huang, X., Aretz, M., Zhang, X.H., Du, Y.S., Luan, T.F., 2019. Upper Viséan coral biostrome in a volcanic-sedimentary setting from the Eastern Tianshan, Northwest China. Palaeogeogr.

Palaeoclimatol. Palaeoecol. 531, 108739.

Iannuzzi, R., Pfefferkorn, H.W., 2002. A Pre-Glacial, Warm-Temperate Floral Belt in Gondwana (Late Visean, Early Carboniferous). Palaios 17, 571–590.

Isaacson, P.E., Díaz-Martínez, E., Grader, G.W., Kalvoda, J., Babek, O., Devuyst, F.X., 2008. Late Devonian-earliest Mississippian glaciation in Gondwanaland and its biogeographic consequences. Palaeogeogr. Palaeoclimatol. Palaeoecol. 268, 126–142.

Isbell, J.L., Henry, L.C., Gulbranson, E.L., Limarino, C.O., Fraiser, M.L., Koch, Z.J., Ciccioli, P.L., Dineen, A.A., 2012. Glacial paradoxes during the late Paleozoic ice age: evaluating the equilibrium line altitude as a control on glaciation. Gondwana Res. 22, 1–19.

Kaiser, S.I., Aretz, M., Becker, R.T., 2016. The global Hangenberg Crisis (Devonian-Carboniferous transition): review of a first-order mass extinction. Geol. Soc. London Spec. Publ. 423, 387–437.

Kawamura, T., 1989. Depositional facies of the Visean (Carboniferous) limestones in the South Kitakami Terrane, northeastern Japan. In: Taira, A., Masuda, F. (Ed.), Sedimentary Facies in the Active Plate Margin. Terra Scientific Publishing co., Tokyo, pp. 377–391.

Kershaw, S., 1994. Classification and geological significance of biostromes. Facies 31, 81–92.

Kiessling, W., Flügel, E., Golonka, J., 1999. Paleoreef Maps: Evaluation of a Comprehensive Database on Phanerozoic Reefs. Am. Assoc. Pet. Geol. Bull. 83, 1552–1587.

Kiessling, W., Flügel, E., Golonka, J., 2000. Fluctuations in the carbonate production of Phanerozoic reefs. In: Insalaco, E., Skelton, P.W., Palmer, T.J. (Ed.), Carbonate Platform Systems: Components and Interactions. Geol. Soc. Lond., Spec. Publ. 178, 191–215.

Kiessling, W., 2002. Secular variations in the Phanerozoic reef systems. In: Kiessling, W., Flügel,

E., Golonka, J. (Ed.), Phanerozoic reef patterns. SEPM Spec. Publ. 72, 625–690.

Kiessling, W., 2009. Geologic and biologic controls on the evolution of reefs. Annu. Rev. Ecol. Evol. Syst. 40, 173–192.

Kiessling, W., Simpson, C., Foote, M., 2010. Reefs as Cradles of Evolution and Sources of Biodiversity in the Phanerozoic. Science 327, 196–198.

Kopaska-Merkel, D.C., Mann, S.D., Pashin, J.C., 2013. Sponge-microbial mound facies, in Mississippian Tuscumbia Limestone, Walker County Alabama. Am. Assoc. Pet. Geol. Bull. 11, 1871–1893.

Korn, D., Ilg, A., 2008. AMMON. http://www.wahre-staerke.com/ammon/.

Lee, J.H., Chen, J.T., Chough, S.K., 2015. The middle-late Cambrian reef transition and related geological events: a review and new view. Earth Sci. Rev. 145, 66–84.

Lees, A., Miller, J., 1985. Facies variations in Waulsortian buildups: part 2. Mid-Dinantian buildups from Europe and North America. J. Geol. 20: 159–180.

Lees, A., Miller, J., 1995. Waulsortian Banks. In: Monty, C.V., Bosence, D.W.J., Bridges, P.H., Pratt, B.R. (Ed.), Carbonate mud-mounds, their origin and evolution. Int. Assoc. Sediment. Spec. Publ. 23, 191–271.

Limarino, C.O., Cesari, S., Spalletti, L.A., Taboada, A.C., Isbell, J.L., Geuna, S., Gulbranson, E.L., 2014. A paleoclimatic review of southern South America during the late Paleozoic: a record from icehouse to extreme greenhouse conditions. Gondwana Res. 25, 1396–1421.

Lord, E.K., Walker, S.E., Aretz, M., 2011. Mississippian (Serpukhovian) framework reef in Northwestern Georgia, USA. Kölner Forum Geol. Paläont. 19, 100–101.

Maharjan, D., Jiang, G., Peng, Y., Henry, R.A., 2018a. Paired carbonate–organic carbon and

nitrogen isotope variations in Lower Mississippian strata of the southern Great Basin, western United States. Palaeogeogr. Palaeoclimatol. Palaeoecol. 490, 462–472.

Maharjana, D., Jiang, G.Q., Peng, Y.B., Nicholla, M.J., 2018b. Sulfur isotope change across the Early Mississippian K-O (Kinderhookian-Osagean) $\delta^{13}C$ excursion. Earth Planet. Sci. Lett. 494, 202–215.

Martindale, R.C., Foster, W.J., Velledits, F., 2018. The survival, recovery, and diversification of metazoan reef ecosystems following the end-Permian mass extinction event. Palaeogeogr. Palaeoclimatol. Palaeoecol. 513, 100–115.

McGhee, G.R., Clapham, M.E., Sheehan, P.M., Bottjer, D.J., Droser, M.L., 2013. A new ecological-severity ranking of major Phanerozoic biodiversity crises. Palaeogeogr. Palaeoclimatol. Palaeoecol. 370, 260–270.

Mii, H.S., Grossman, E.L., Yancey, T.E., 1999. Carboniferous isotope stratigraphies of North America: Implications for Carboniferous paleoceanography and Mississippian glaciation. Geol. Soc. Am. Bull. 111, 960–973.

Montañez, I.P., Norris, R.D., Algeo, T.J., Chandler, M.A., Johnson, K.R., Kennedy, M.J., Kent, D.V., Kiehl, J.T., Kump, L.R., Ravelo, A.C., Turekian, K.K., 2011. Understanding Earth's Deep Past: Lessons for Our Climate Future. National Academy of Sciences Press, Washington, DC, pp. 1–193.

Mundy, D.J.C., 1994. Microbialite-sponge-bryozoan-coral framestones in Lower Carboniferous (Late Viséan) buildups of Northern England (UK). In: Embry, A.F., Beauchamp, B., Glass, D.J. (Ed.), Pangea: Global Environments & Resources. Can. Soc. Petro. Geol. Mem. 17, 713–729.

Nakazawa, T., 2011. Carboniferous Reef Succession of the Panthalassan Open-Ocean Setting: Example from Omi Limestone, Central Japan. Facies 44, 183–210.

Nance, R.D., Linnemann, U., 2008. The Rheic Ocean: origin, evolution and significance. GSA Today 18, 4–12.

Ogar, V.V., 2012. Carboniferous buildups in the Donets Basin (Ukraine). Geol. Belg. 15, 340-349.

Ogg, J.G., Ogg, G.M., Gradstein, F.M. 2016. A Concise Geologic Time Scale. Elsevier B.V. Press, Boston, pp. 1–234.

Penny, A.M., Wood, R., Curtis, A., Bowyer, F., Tostevin, R., Hoffman, K.-H., 2014. Ediacaran metazoan reefs from the Nama Group, Namibia. Science 344, 1504–1506.

Poty, E., 1999. Famennian and Tournaisian recoveries of shallow water Rugosa following late Frasnian and late Strunian major crises, southern Belgium and surrounding areas, Hunan (South China) and the Omolon region (NE Siberia). Palaeogeogr. Palaeoclimatol. Palaeoecol. 154, 11–26.

Poty, E., Hance, L., Lees, A., Hennebert, M., 2002. Dinantian lithostratigraphic units (Belgium). Geol. Bel. 4, 69–93.

Poty, E., Devuyst, F.-X., Hance, L., 2006. Upper Devonian and Mississippian foraminiferal and rugose coral zonations of Belgium and northern France: a tool for Eurasian correlations. Geol. Mag. 143, 829–857.

Poty, E., Aretz, M., Denayer, J., 2011. Field trip 3: Uppermost Devonian and Lower Carboniferous of Southern Belgium. Köl. Fo. Geol. Pal. 20, 99–150.

Poty, E., 2016. The Dinantian (Mississippian) succession of southern Belgium and surrounding areas: stratigraphy improvement and inferred climate reconstruction. Geol. Belg. 19,

177–200.

Powell, M.G., Schöne, B.R., Jacob, D.E., 2009. Tropical marine climate during the late Paleozoic ice age using trace element analyses of brachiopods. Palaeogeogr. Palaeoclimatol. Palaeoecol. 280, 143–149.

Qiao, L., Shen, S.Z., 2015. A global review of the Late Mississippian (Carboniferous) Gigantoproductus (Brachiopoda) faunas and their paleogeographical, paleoecological, and paleoclimatic implications. Palaeogeogr. Palaeoclimatol. Palaeoecol. 420, 128–137.

Raymond, A., Kelley, P.H., Lutken, C.B., 1990. Dead by degrees: Articulate brachiopods, paleoclimate and the mid-Carboniferous extinction. Palaios 5, 111–123.

Riding, R., 2002. Structure and composition of organic reefs and carbonate mud mounds: concepts and categories. Earth-Sci. Rev. 58, 163–231.

Riding, R., 2006. Microbial carbonate abundance compared with fluctuations in metazoan diversity over geological time. Sediment. Geol. 185, 229–238.

Rodríguez, S., Arribas, M.E., Falces, S., Morena-Eiris, E., de la Pena, J., 1994. The Siphonodendron limestone of the Los Santos de Maimona basin: development of an extensive reef-flat during the Viséan in Ossa Morena, Spain. Courier Forschungsinstitut Senckenberg 172, 203–214.

Rodríguez, S., Somerville, I.D., Said, I., Cózar, P., 2012. Late Viséan coral fringing reef at Tiouinine (Morocco): implications for the role of rugose corals as building organisms in the Mississippian. Geol. J. 47, 462–476.

Rodríguez, S., Said, I., Somerville, I.D., Cózar, P., Coronado, I., 2016. Serpukhovian coral assemblages from Idmarrach and Tirhela Formations (Adarouch, Morocco). Geol. Bel. 19,

29–42.

Saltzman, M.R., González, L.A., Lohmann, K.C., 2000. Earliest Carboniferous cooling step triggered by the Antler orogeny? Geology 28, 347–350.

Saltzman, M.R., Groessens, E., Zhuravlev, A.V., 2004. Carbon cycle models based on extreme changes in $\delta^{13}C$: an example from the lower Mississippian. Palaeogeogr. Palaeoclimatol. Palaeoecol. 213, 359–377.

Saltzman, M.R., Thomas, E., 2012. Chapter 11—Carbon isotope stratigraphy. In: Gradstein, F., Ogg, J., Schmitz, M., Ogg, G. (Eds.), The Geologic Time Scale 2012. Elsevier B.V. Press, Boston, pp. 207–232.

Shen, J.W., Webb, G.E., 2005. Metazoan-microbial framework fabrics in a Mississippian (Carboniferous) coral-sponge-microbial reef, Monto, Queensland, Australia. Sediment Geol. 178, 113–133.

Shen, J.W., Webb, G.E., 2008. The role of microbes in reef-building communities of the Cannindah limestone (Mississippian), Monto region, Queensland, Australia. Facies 54, 89–105.

Shen, S.Z., Jin, J., Shi, G.R., 2016. Ecosystem evolution in deep time: Evidence from the rich Paleozoic fossil records of China. Palaeogeogr. Palaeoclimatol. Palaeoecol. 448: 1-3.

Siegmund, H., Trappe, J., Oschmann, W., 2002. Sequence stratigraphic and genetic aspects of the Tournaisian “Liegender Alaunschiefer”. Geol. Rundsch. 91, 934–949.

Smith, L.B., Read, J.F., 2000. Rapid onset of late Paleozoic glaciation on Gondwana: evidence from Upper Mississippian strata of the Midcontinent, United States. Geology 28, 279–282.

Somerville, I.D., Rodríguez, S., 2007. Rugose coral associations from the late Viséan

(Carboniferous) of Ireland, Britain and SW Spain. In: Hubmann, B., Piller, W.E. (Ed.), Fossil Corals and Sponges, Proceedings of the 9th International Symposium on Fossil Cnidaria and Porifera, Graz, 2003. Austrian Academy of Sciences, Schriftenreihe der Erdwissenschaftlichen Kommissionen 17, Vienna, pp. 329–351.

Somerville, I.D., 2008. Biostratigraphic zonation and correlation of Mississippian rocks in Western Europe: some case studies in the late Viséan/Serpukhovian. Geol. J. 43, 209–240.

Song, H.J., Wignall, P.B., Chen, Z.Q., Tong, J.N., Bond, D.P.G., Lai, X.L., Zhao, X.M., Jiang, H.S., Yan, C.B., Niu, Z.J., Chen, J., Yang, H., Wang, Y.B., 2011. Recovery tempo and pattern of marine ecosystems after the end-Permian mass extinction. Geology 39, 739–742.

Stanley, Jr,G.D., 2006. Photosymbiosis and the evolution of modern coral reefs. Science 312, 857–858.

Stanley, Jr,G.D., Lipps, J.H., 2011. Photosymbiosis: the driving force for reef success and failure. Paleontol. Soc. Paper 17, 33–60.

Talent, J.A., 1988. Organic reef-building: Episodes of extinction and symbiosis? Senckenb. lethaea, 69, 315–368.

Veizer, J., Ala, D., Azmy, K., Bruckschen, P., Buhl, D., Bruhn, F., Carden, G.A.F., Diener, A., Ebneth, S., Godderis, Y., Jasper, T., Korte, G., Pawellek, F., Podlaha, O.G., Strauss, H., 1999. $^{87}Sr/^{86}Sr$, $\delta^{13}C$ and $\delta^{18}O$ evolution of Phanerozoic seawater. Chem. Geol. 161, 59–88.

Wang, X.D., Hu, K.Y., Qie, W.K., Sheng, Q.Y., Chen, B., Lin, W., Yao, L., Wang, Q.L., Qi, Y.P., Chen, J.T., Liao, Z.T., Song, J.J., 2019. Carboniferous integrative stratigraphy and time scale of China. Sci. China Earth Sci. 62, 135–153.

Waters, C.N., Haslam, R.B., Cózar, P., Somerville, I.D., Millward, D., Woods, M. 2019.

Mississippian reef development in the Cracoe Limestone Formation of the southern Askrigg Block, North Yorkshire, UK. P. Yorks. Geol. Soc. 61, 179-196.

Webb, G.E., 1989. Late Visean coral-algal bioherms from the Lion Creek Formation of Queensland, Australia. Eleventh Int. Congr. Carboniferous Strat. Geol. 3, 282–295.

Webb, G.E., 1994. Non-Waulsortian Mississippian bioherms: a comparative analysis. In: Embry, A.F., Beauchamp, B., Glass, D.J. (Ed.), Pangea: Global Environments & Resources. Can. Soc. Petro. Geol. Mem. 17, 701–712.

Webb, G.E., 1998. Earliest known Carboniferous shallow-water reefs, Gudman Formation (Tn1b), Queensland, Australia: Implications for Late Devonian reef collapse and recovery. Geology 26, 951–954.

Webb, G.E., 1999. Youngest Early Carboniferous (Late Viséan) shallow-water patch reefs in Eastern Australia (Rockhampton Group, Queensland): Combining quantitative micro- and macro-Scale data. Facies 41, 111–140.

Webb, G.E., 2002. Latest Devonian and Early Carboniferous reefs: depressed reef building after the Middle Paleozoic collapse. In: Kiessling, W., Flügel, E., Golonka, J. (Ed.), Phanerozoic reef patterns. SEPM Spec. Publ. 72, 239–270.

Webb, G.E., 2005. Quantitative analysis and paleoecology of earliest Mississippian microbial reefs, lowermost Gudman formation, Queensland, Australia: not just post-disaster phenomena. J. Sediment. Res. 75, 875–894.

Wignall, P.B., Twitchett, R.J., 2002. Extent, duration, and nature of the Permian-Triassic superanoxic event. Geol. Soc. Am. Spec. Paper 356, 395–413.

Wood, R., 1999. Reef Evolution. Oxford University Press, Oxford, pp. 1–414.

Yao, L. Qie, W.K., Luo, G.M., Liu, J.S., Algeo, T.J., Bai, X., Yang, B., Wang, X.D., 2015. The TICE event: Perturbation of carbon-nitrogen cycles during the mid-Tournaisian (Early Carboniferous) greenhouse-icehouse transition. *Chem. Geol.* **401**, 1–14.

Yao, L., Wang, X.D., 2016. Distribution and evolution of Carboniferous reefs in South China. Palaeoworld 25, 362–372.

Yao, L., Aretz, M., Chen, J.T., Webb, G.E., Wang, X.D., 2016a. Global microbial carbonate proliferation after the end-Devonian mass extinction: Mainly controlled by demise of skeletal bioconstructors. Sci. Rep. 6, 39694.

Yao, L., Wang, X.D., Lin, W., Li, Y., Kershaw, S., Qie, W.K., 2016b. Middle Viséan (Mississippian) coral biostrome in central Guizhou, south-western China and its palaeoclimatological implications. Palaeogeogr. Palaeoclimatol. Palaeoecol. 448: 179–194.

Yao, L., Aretz, M., Li, Y., Wang, X.D., 2016c. Gigantoproductid brachiopod storm shell beds in the Mississippian of South China: implications for their paleoenvironmental and paleogeographical significances. Geol. Belg. 19, 57–67.

Yao, L., Aretz, M., Chen, J.T., Qi, Y.P., 2019. Earliest Carboniferous stromatolites from the Qianheishan Formation, Dashuigou section, northwestern China: Implications for microbial proliferation after the end-Devonian mass extinction. Geol. J. 1–16. https://doi.org/10.1002/gj.3588.

Zapalski, M.K., 2014. Evidence of photosymbiosis in Palaeozoic tabulate corals. Proc. R. Soc. B. 281, 20132663.

Zapalski, M.K., Nowicki, J., Jakubowicz, M., Berkowski, B., 2017a. Tabulate corals across the Frasnian/Famennian boundary: architectural turnover and its possible relation to ancient

photosymbiosis. Palaeogeogr. Palaeoclimatol. Palaeoecol. 487, 416–429.

Zapalski, M.K., Wrzołek, T., Skompski, S., Berkowski, B., 2017b. Deep in shadows, deep in time: the oldest mesophotic coral ecosystems from the Devonian of the Holy Cross Mountains (Poland). Coral Reefs 36, 847–860.

Zapalski, M.K., Berkowski, B., 2019. The Silurian mesophotic coral ecosystems: 430 million years of photosymbiosis. Coral Reefs 38, 137–147.

Table caption

Table 1. Calculated proxies for bioconstruction abundance, including assumed value of bioconstruction width and thickness, and biotic content proxy of different bioconstruction types.

Figure captions

Fig. 1. Palaeogeographic location of global Mississippian bioconstructions. (A) Early Visean bioconstructions. (B) Middle Visean bioconstructions. (C) Late Visean bioconstructions. (D) Late Visean coral bioconstructions in South China Block (the red rectangle in Fig. 1C, note that is rotated ~90° counter-clockwise relative to its modern orientation). (E) Early Serpukhovian bioconstructions. (F) Late Serpukhovian bioconstructions. The base map is revised from Blakey (2011). Abbreviations: Al, Alabama, USA; Ar, Arkansas, USA; Au, Australia; BB, Béchar Basin, Algeria; Be, Belgium; Ca, Canada; DB, Donets Basin, Ukraine; DQGX, Dian-Qian-Gui-Xiang platform; Fr, France; GDZ, Gandongzi section; Jp, Japan; IM, Inner Mongolia, China; Ir, Ireland; LP, Langping isolated platform; Mo, Morocco; Mon, Monto, Queensland, Australia; NG, Northwestern Georgia, USA; NS, Nova Scotia, Canada; NWC, Northwestern China; Po, Poland; QG, Qian-Gui Basin; Sa, Saskatchewan, Canada; SNB, southern New Brunswick, Canada; Sp, Spain; SC, South China; Tu, Turkey; TU: Timan-Ural, Russia; UK, United Kingdom; Ukr, Ukraine; XD, Xiadong section; YS, Yashui section.

Fig. 2. Mississippian stratigraphic frameworks for sections at Yashui, Guizhou Province and Langping, Guangxi Province in South China with reef locations, and their correlations with coeval stratigraphic frameworks in Western Europe, North America and globe. Revised based on

Somerville (2008), Hance et al. (2011) and Wang et al. (2019). Abbreviations: B & I, Britain & Ireland; Bel., Belgium; E, Early; L, Late; M, Middle; MFZ, Mississippian foraminiferal zone; W. Euro., Western Europe.

Fig. 3. Field photographs of the Tournaisian microbial reefs and carbonate mud mounds. (A) Early Tournaisian microbial reef from the Gudman Formation, Queensland, Eastern Australia (northeastern margin of Gondwana). The microbial reef (dark-greyish colour) is enbedded into oolitic limestones (lighter grey colour). Reef height is a few metres. (B) Early Tournaisian domal stromatolites from the Qianheishan Formation, Gansu Province, northwestern China (eastern Tianshan orogenic belt between the Siberian and Tarim blocks). (C) Late Tournaisian Waulsortian mud mound from the Leffe Formation near Dinant town, Belgium. Photo provided by J. Denayer. (D) Late Tournaisian Waulsortian-like mud mound from the Long'an Formation, Guangxi Province, South China Block. (E) Thin-section photograph of the core facies of the mud mounds in South China. Abbreviations: B, Bryozoan; Bra, Brachiopod; C, Crinoid; M, Mud; O, Ostracod; SC, Sparry calcite; SS, Sponge spicule; St, Stromatactis structure.

Fig. 4. Field photographs of the Visean coral bioconstructions from Laurussia, Gondwana, Akiyoshi Seamount and South China. (A) Alignment of late Visean microbial-sponge-bryozoan-coral reefs in the Jerada Basin, Morocco (northern margin of Gondwana). The reef sizes are up to several hundred metres in width and several tens of metres in height. (B) Late Visean true coral reef in the Blue Pool Bay section, South Wales, UK (southern shelf of Laurussia). The reef (outlined in red) is 12 m height and few tens of metres wide,

embedded within grainy, bioclastic and oolitic limestones. (C) Colonial rugose coral frameworks from the reef core in the Blue Pool Bay section. (D) Coral-chaetetid biostrome from Little Asby Scar, Cumbria, UK (southern shelf of Laurussia). (E) Patch of coral framework from the late Visean coral-microbial reefs of the Lion Creek Formation, Queensland, Australia (eastern margin of Gondwana). (F) Coral framework in the Akiyoshi seamount carbonates in Japan (western Panthalassic Ocean). Abbreviations: crc, colonial rugose coral; t, tabulate coral.

Fig. 5. Field, polished-slab and thin-section photographs of the late Visean coral reefs and frameworks from the Gandongzi and Xiadong sections in Guangxi Province, and the coral biostromes from the Yashui section in Guizhou Province, South China. (A) Large coral reef in the Gandongzi section. (B) Big colonial rugose coral colony from the Gandongzi coral reef. (C) Coral reef containing attached colonial rugose coral colonies from the Xiadong section. (D) Tabulate coral frameworks in the Gandongzi section. (E) Colonial rugose coral biostromes from the Yashui section. (F) Macroview showing the characteristics of coral reefs containing abundant microbial crusts and sparry calcite cements around coral skeletons, Gandongzi section. (G) Macroview of coral biostrome comprising of abundant micrite and lacking of microbial binding and sparry calcite cementation facies, Yashui section. (H-L) Main builders of coral reefs and biostromes, including colonial rugose corals (*Diphyphyllum*, *Stylostrotion* and *Lithostrotion*), and tabulate corals (*Syringopora*), and microview of the microfacies features of coral reefs (H-K) and coral biostromes (I), which are composed of and lack of microbial and cementation facies, respectively. (M-O) Encrusting biota, including microbes (*Renalcis*), cystoporate bryozoans (*Fistulipora*) and foraminifers (*Tetrataxis*) on coral walls. (P) Asexual budding structure of corals from the coral

reefs and biostromes. Abbreviations: ab, asexual budding; b, bryozoan; br, brachiopod; c, crinoid; ca, calcisphere; cf, coral fragment; crc, colonial rugose coral; *Di*, *Diphyphyllum*; f, foraminifer; *Fi*, *Fistulipora*; g, gastropod; *Li*, *Lithostrotion*; mc, microbial crust; is, internal space; o, ostracod; p, peloid; *Re*, *Renalcis*; sc, sparry calcite; *Si*, *Siphonodendron*; *St*, *Stylostrotion*; *Sy*, *Syringopora*; t, tabulate coral; *Te*, *Tetrataxis*.

Fig. 6. Field photographs of the Serpukhovian coral bioconstructions. (A) Late Serpukhovian coral biostrome from the Dahuanggou Formation, western Inner Mongolia, northwestern China. (B) Massive colonial rugose coral (MCRC) colony from the yellow rectangle area of the biostrome in Fig. 6A. (C) Late Serpukhovian coral biostrome from the Djenien Formation, Béchar Basin, Algeria. (D) Fasciculate colonial rugose coral (FCRC) colony from the biostrome in Fig. 6C. Photos C and D from Atif et al. (2016).

Fig. 7. Variations in the abundance of reefs and reef builders and metazoan reef evolutionary pattern from the Late Devonian to Mississippian. Profiles of reef and reef-builder abundance are based on Supplementary Table 3. Abbreviations: E, Early; F-F, Frasnian-Famennian; L, Late; M, Middle; MFZ, Mississippian foraminiferal zone; MRG, Metazoan "reef gap" phase; MRR, Metazoan reef re-establishment phase; MRP, Metazoan reef proliferation phase; Serp., Serpukhovian.

Fig. 8. Triangular plots showing the correlation between reef-builder abundance of coral, microbe, bryozoan and sponge (A), and the correlation between skeletal reef-builder abundance of coral,

bryozoan and sponge (B) from the middle Visean to late Serpukhovian. Plots are compiled based on the data of quantitative values of different biotic components from Supplementary Table 3. Hollow symbols represent the average value of reef builders during time slices of the middle Visean (MV), early Asbian (EA), late Asbian (LA), early Brigantian (EB), late Brigantian (LB), early Serpukhovian (ES) and late Serpukhovian (LA) in ascending order. Symbol morphology and colour (correspond to Fig. 7) stands for relevant stage and biotic composition respectively, and its size shows occurrence frequency (OF).

Fig. 9. Global changes in diversity of nektonic and benthic faunas, and abundance of reef corals and skeletal reefs, showing the marine ecosystem resurgence (MER) (blue band) during the Mississippian. Ammonoid, foraminifer and brachiopod diversity from Raymond et al. (1990), Korn and Ilg (2008), Groves and Wang (2009) and Qiao and Shen (2015). High-resolution of rugose coral diversity is based on our own data from Europe. Reef coral and skeletal reef abundance are from Fig. 7 in this study. Abbreviations: E: Early; GN, Genera number; HMEE: Hangenberg mass extinction event; L: Late; M: Middle; MER, Marine ecosystem resurgence; MFZ: Mississippian foraminiferal zone; Serp.: Serpukhovian; SN, Species number; WA, Weighted abundance.

Fig. 10. Variations in carbon and strontium isotope ratios, glacial distribution and adjusted tropical sea-surface temperature (SST) from the Late Devonian to Mississippian. Carbon isotopic trend is drawn according to the data from Saltzman (2012). Strontium isotopic trend is compiled based on the data from Bruckschen et al. (1995), Bruckschen et al. (1999), Veizer et al. (1999) and Chen et

al. (2018). Glacial distribution profile is derived from information in Supplementary Table 1. Tropical SST curve (red) is from Ogg et al. (2016), with the grey background showing its trend changes. Abbreviations: E, Early; L, Late; M, Middle; MFZ, Mississippian foraminiferal zone; Serp., Serpukhovian; TICE, Tournaisian carbon isotope excursion.

Fig. 11. Comparison of the metazoan reef-recovery intervals between the middle-late (M-L) Cambrian, Mississippian, and Triassic after the early-middle (E-M) Cambrian, Frasnian-Famennian (F-F) and Hangenberg, and Permian-Triassic (P-T) mass extinctions, respectively. The blue bar width represents relatively metazoan reef abundance. The reef-recovery pattern during the E-M Cambrian and P-T extinction transisitons, was drew mainly based on Lee et al. (2015) and Martindale et al. (2018), respectively.

Fig. 12. Comparison between the abundance of reefs and reef builders, stromatoporoid and rugose coral diversity, carbon and strontium isotope ratios, tropical sea-surface temperature (SST), and glacial distribution from the Late Devonian to Mississippian. Profiles of reef and reef-builder abundance are from Fig. 7. Global generic diversity of the Late Devonian stromatoporoids and rugose corals is compiled from the Palaeobiology Database (https://www.paleobiodb.org/#/). Mississippian colonial rugose coral diversity (with high resolution both for genera and species) is our own data. Carbon and strontium isotopic trend, tropical SST curve, and glacial distribution profiles are from Fig 10. Abbreviations: E, Early; F-F, Frasnian-Famennian; L, Late; M, Middle; MFZ, Mississippian foraminiferal zone; MRG, Metazoan “reef gap” phase; MRR, Metazoan reef re-establishment phase; MRP, Metazoan reef proliferation phase; Serp., Serpukhovian; TICE,

Tournaisian carbon isotope excursion.

Table

Assumed value	Bioconstruction width	Bioconstruction thickness	Bioconstruction type	Biotic content proxy
1	<10 m	<10 m	Organic reef	1
2	10—100 m	10—100 m	Reef mound	0.7
3	101—1000 m	101—500 m		
4	>1000 m	>500 m	Biostrome	1

Table 1.

Figures

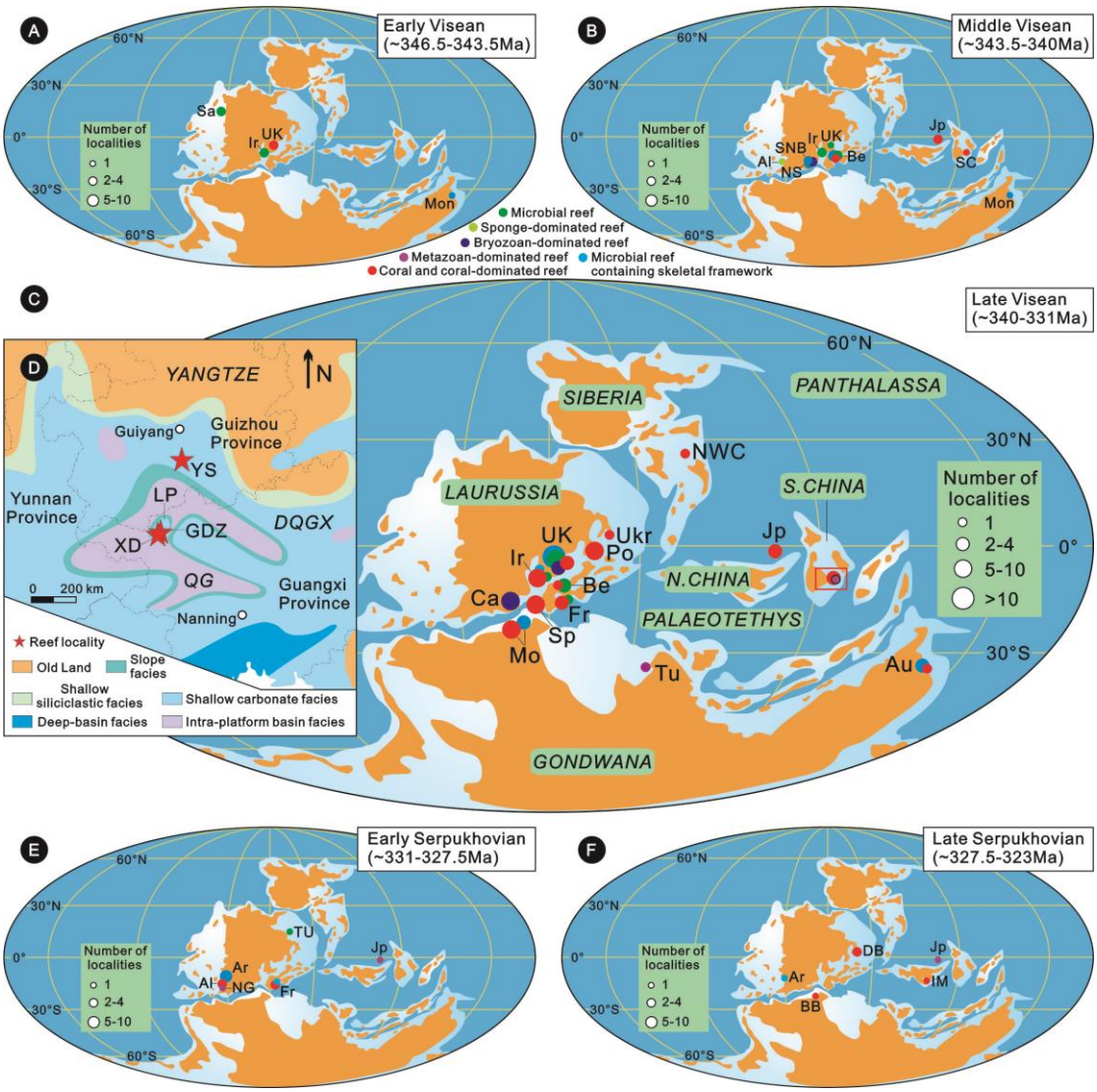

Fig. 1.

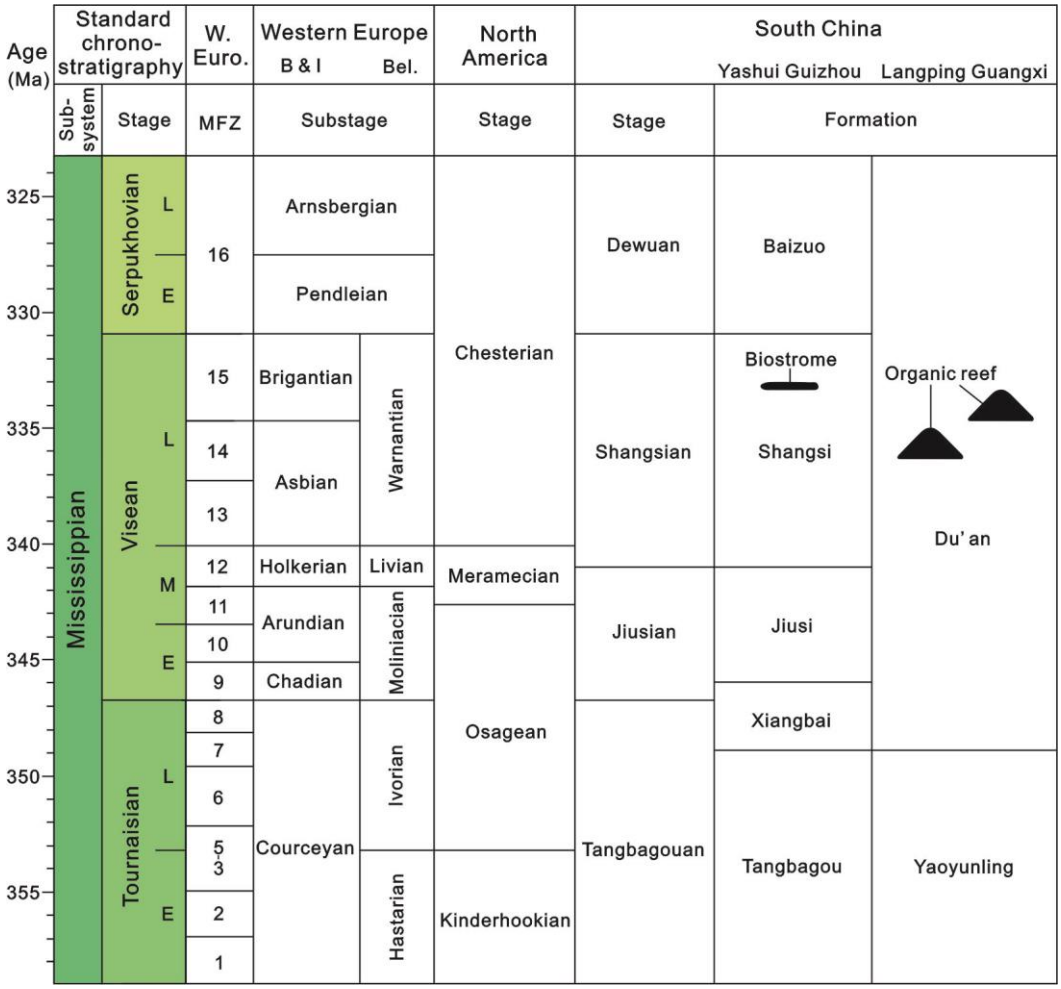
Age (Ma)
Standard chrono-stratigraphy
W. Euro.
Western Europe
B & I
Bel.
North America
South China
Yashui Guizhou
Langping Guangxi
Sub-system
Stage
MFZ
Substage
Stage
Stage
Formation
325
330
335
340
345
350
355
Mississippian
Serpukhovian
Visean
Tournaisian
L
E
L
M
E
L
E
16
15
14
13
12
11
10
9
8
7
6
5
3
2
1
Arnsbergian
Pendleian
Brigantian
Asbian
Holkerian
Arundian
Chadian
Courceyan
Warnantian
Livian
Moliniacian
Ivorian
Hastarian
Chesterian
Meramecian
Osagean
Kinderhookian
Dewuan
Shangsian
Jiusian
Tangbagouan
Baizuo
Biostrome
Shangsi
Jiusi
Xiangbai
Tangbagou
Organic reef
Du' an
Yaoyunling

Fig. 2.

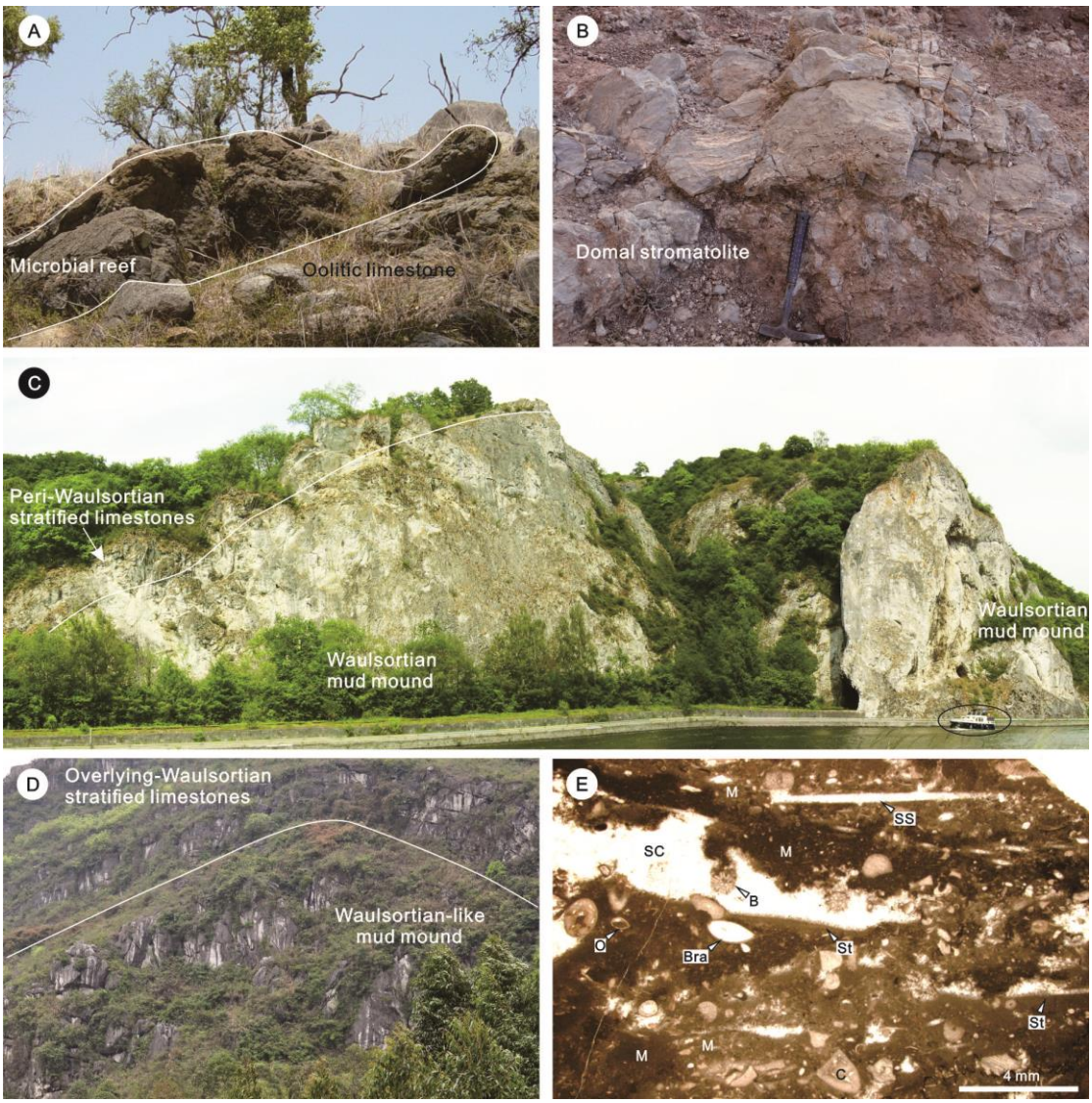
A
Microbial reef
Oolitic limestone
B
Domal stromatolite
C
Peri-Waulsortian
stratified limestones
Waulsortian
mud mound
Waulsortian
mud mound
D
Overlying-Waulsortian
stratified limestones
Waulsortian-like
mud mound
E
M
SS
SC
M
B
O
Bra
St
St
M
M
C
4 mm

Fig. 3

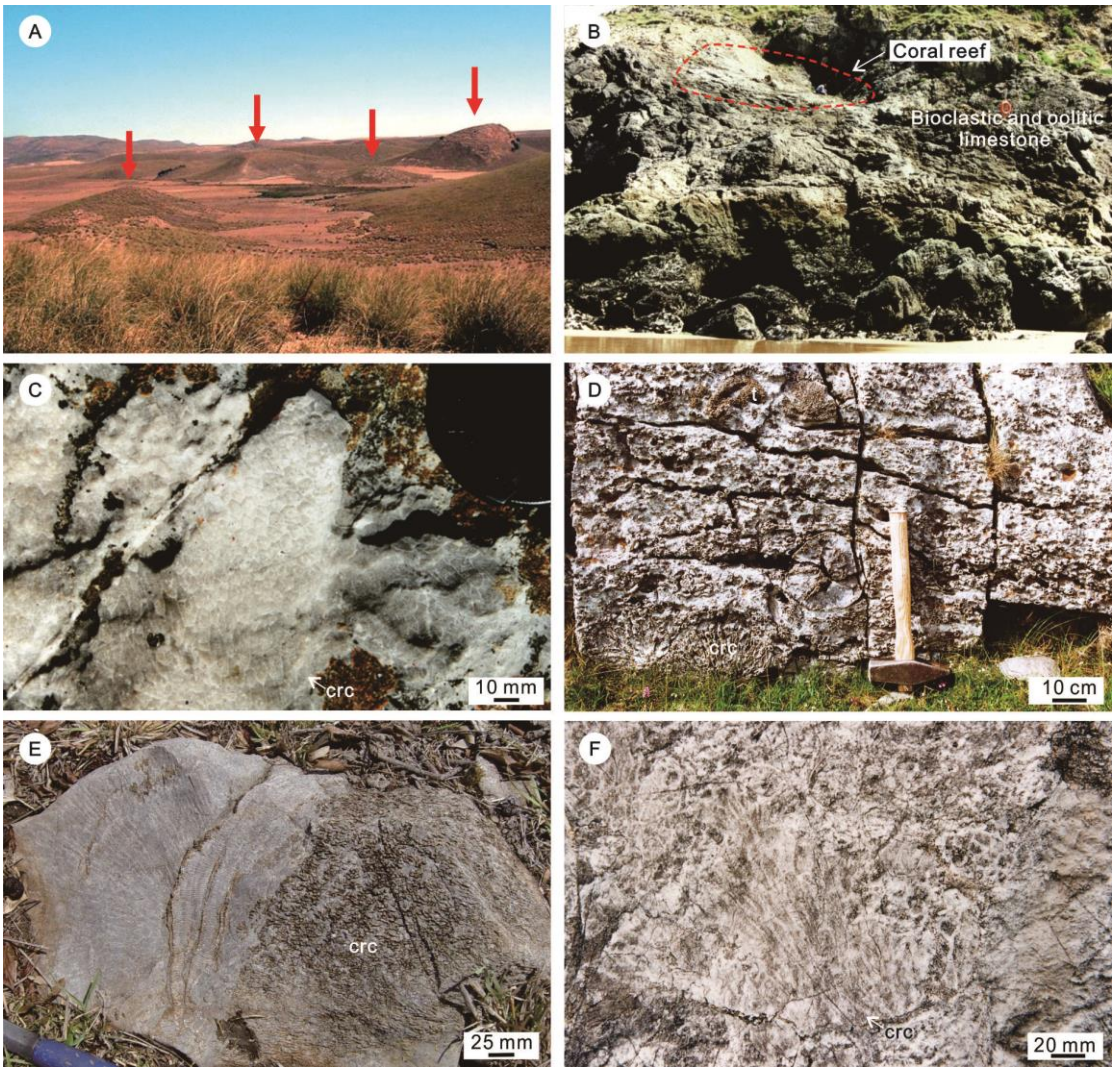
A
B
Coral reef
Bioclastic and oolitic limestone
C
crc
10 mm
D
crc
10 cm
E
crc
25 mm
F
crc
20 mm

Fig. 4.

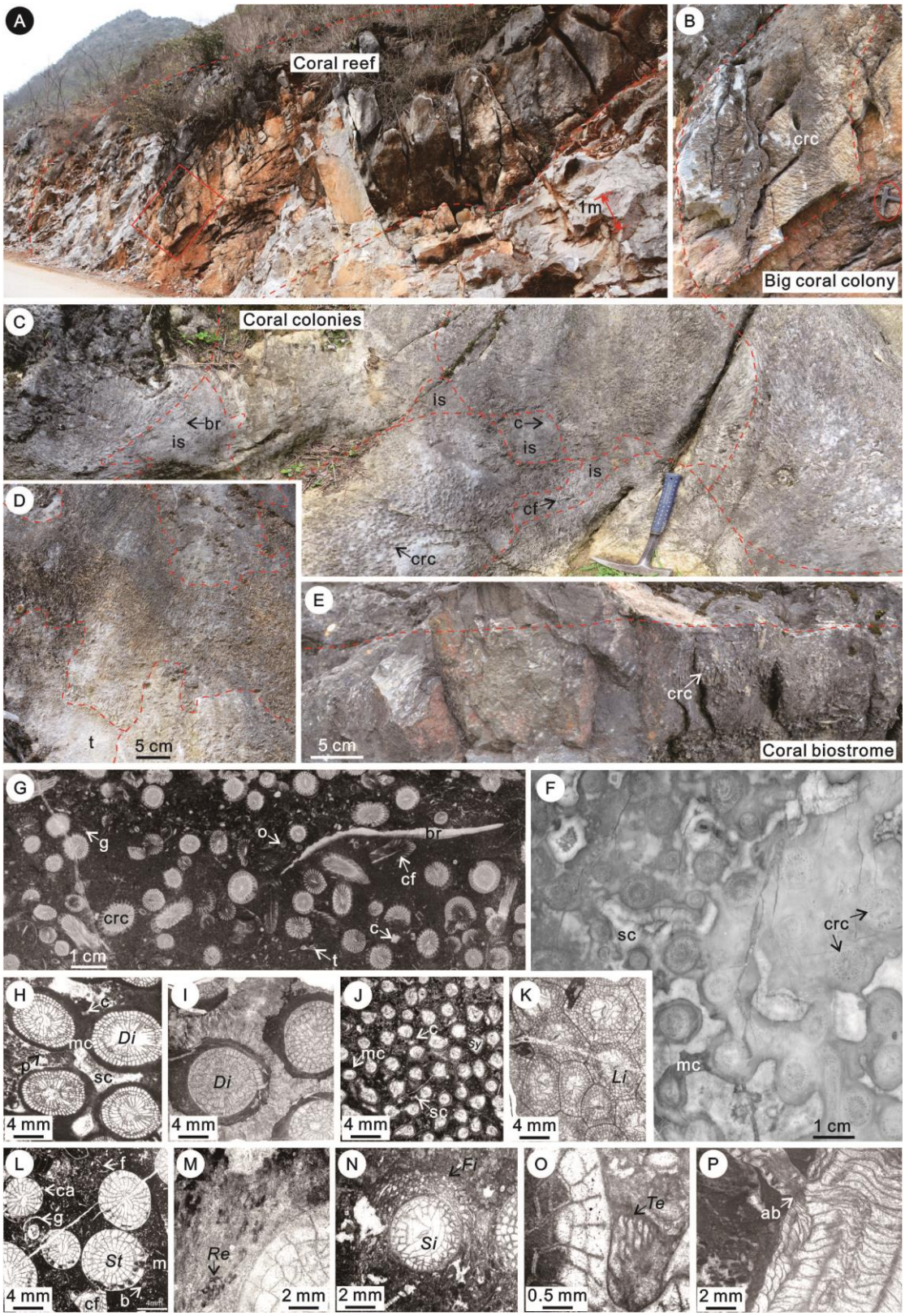
A
Coral reef
1m
B
crc
Big coral colony
C
Coral colonies
br
is
is
c
is
is
cf
crc
D
t
5 cm
E
crc
5 cm
Coral biostrome
G
g
o
br
cf
crc
c
t
1 cm
F
sc
crc
mc
1 cm
H
c
Di
mc
p
sc
4 mm
I
Di
4 mm
J
c
mc
sy
sc
4 mm
K
Li
4 mm
L
f
ca
g
St
m
cf
b
4 mm
M
Re
2 mm
N
Fl
Si
2 mm
O
Te
0.5 mm
P
ab
2 mm

Fig. 5.


A
Coral biostrome
MCRC
B
5 cm
C
Coral biostrome
D
5 cm
FCRC

Fig. 6.

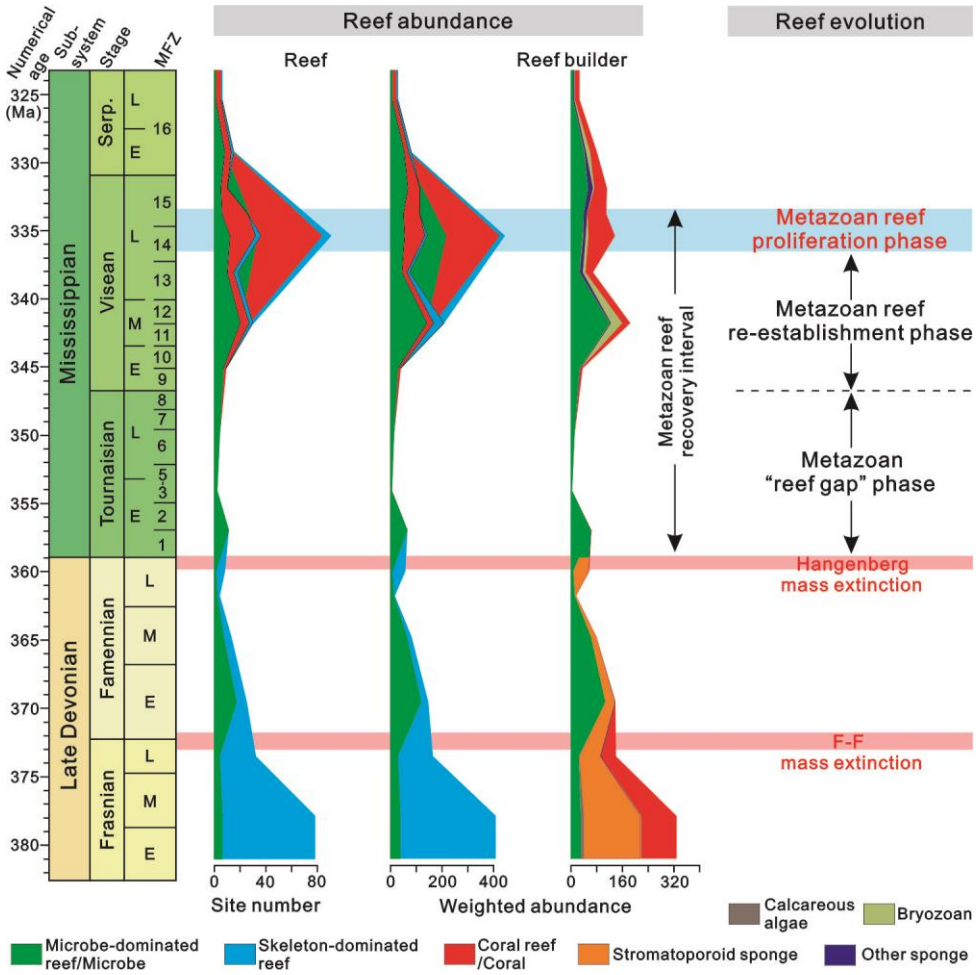
Numerical age (Ma)
Sub-system
Stage
MFZ
Reef abundance
Reef
Reef builder
Reef evolution
Mississippian
Late Devonian
Serp.
Viséan
Tournaisian
Famennian
Frasnian
Site number
Weighted abundance
Metazoan reef proliferation phase
Metazoan reef re-establishment phase
Metazoan "reef gap" phase
Metazoan reef recovery interval
Hangenberg mass extinction
F-F mass extinction
Microbe-dominated reef/Microbe
Skeleton-dominated reef
Coral reef /Coral
Stromatoporoid sponge
Other sponge
Calcareous algae
Bryozoan

Fig. 7.

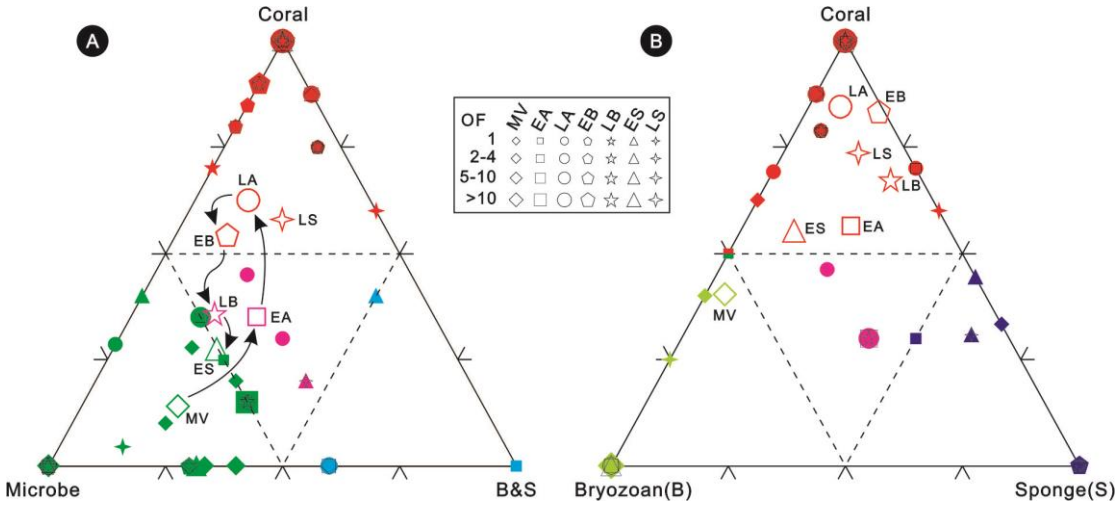
A
Coral
LA
LS
EB
LB
EA
ES
MV
Microbe
B&S
B
Coral
LA
EB
LS
LB
ES
EA
MV
Bryozoan(B)
Sponge(S)
OF
MV
EA
LA
EB
LB
ES
LS
1
2-4
5-10
>10

Fig. 8.

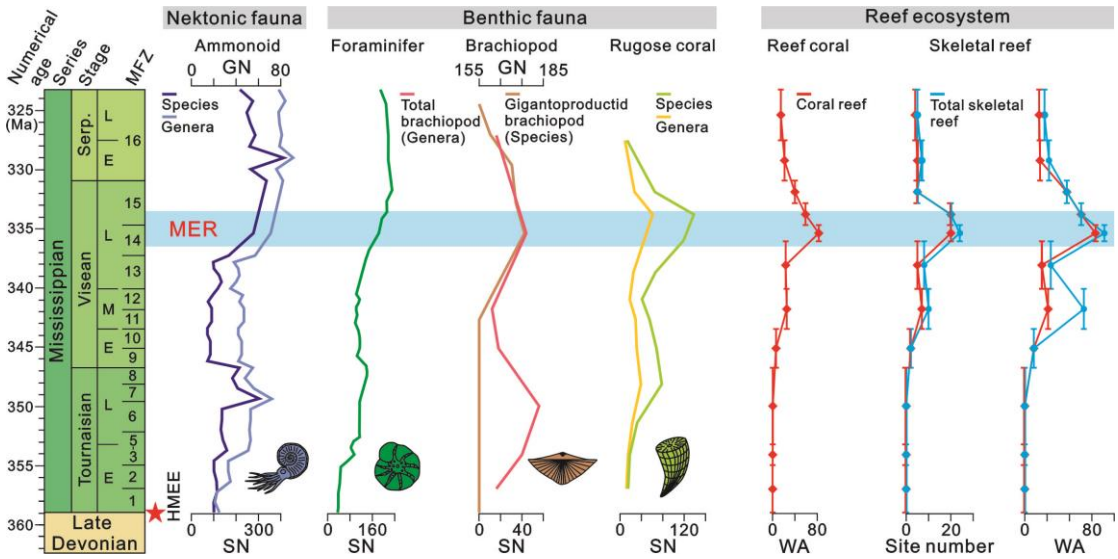
Numerical age
Series
Stage
MFZ
Nektonic fauna
Ammonoid
GN
Benthic fauna
Foraminifer
Brachiopod
Rugose coral
Reef ecosystem
Reef coral
Skeletal reef
Species
Genera
Total brachiopod (Genera)
Gigantoproductid brachiopod (Species)
Coral reef
Total skeletal reef
MER
HMEE
Mississippian
Late Devonian
Serp.
Visean
Tournaisian
SN
WA
Site number

Fig. 9.

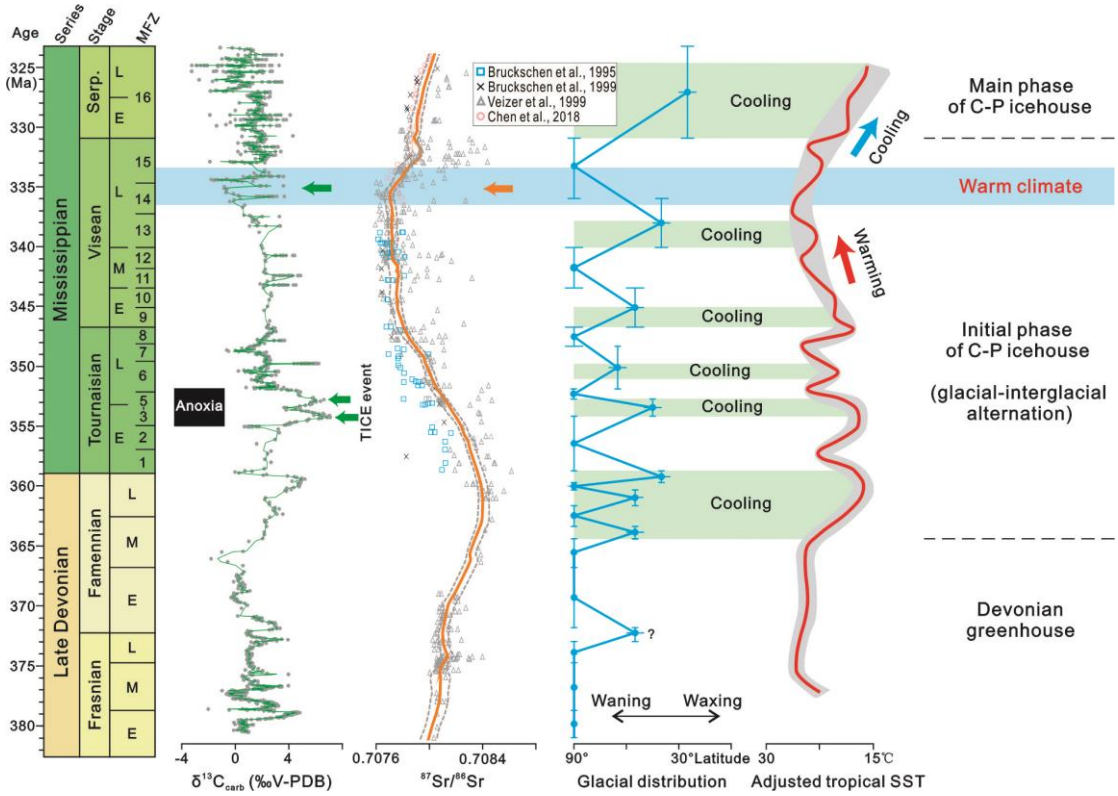
Age
Series
Stage
MFZ
Mississippian
Late Devonian
Serp.
Visean
Tournaisian
Famennian
Frasnian
Anoxia
TICE event
Bruckschen et al., 1995
Bruckschen et al., 1999
Veizer et al., 1999
Chen et al., 2018
Cooling
Warming
Main phase of C-P icehouse
Warm climate
Initial phase of C-P icehouse
(glacial-interglacial alternation)
Devonian greenhouse
Waning
Waxing
δ13Carb (‰V-PDB)
87Sr/86Sr
Glacial distribution
Adjusted tropical SST
90°
30°Latitude
30
15℃

Fig. 10.

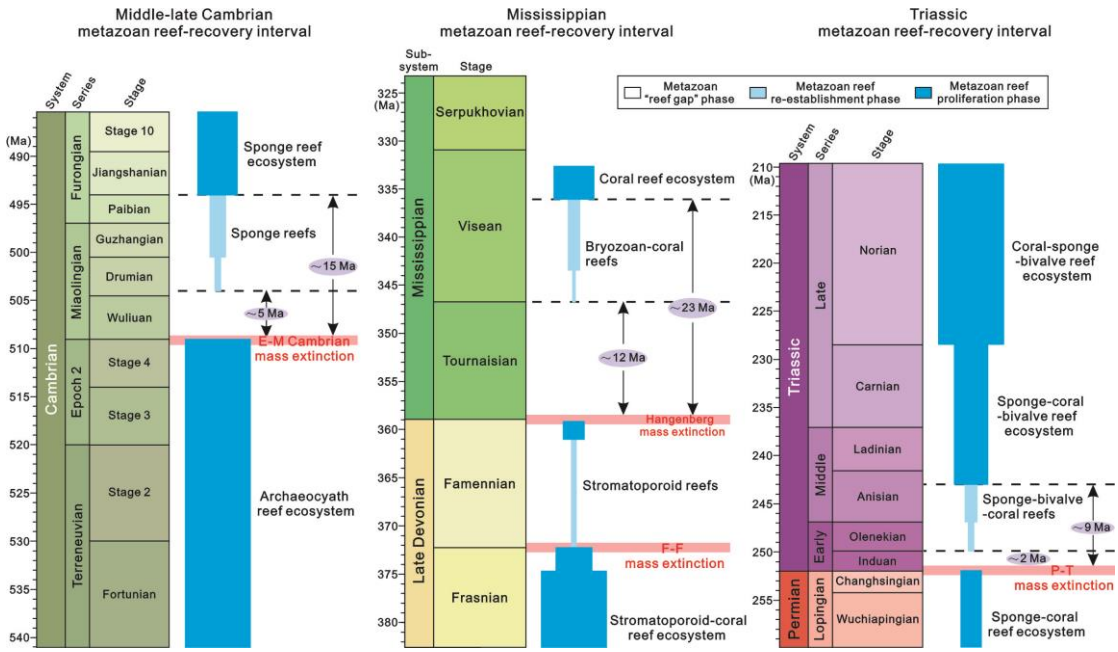
Middle-late Cambrian metazoan reef-recovery interval
Mississippian metazoan reef-recovery interval
Triassic metazoan reef-recovery interval
Metazoan "reef gap" phase
Metazoan reef re-establishment phase
Metazoan reef proliferation phase
Cambrian
Furongian
Miaolingian
Epoch 2
Terreneuvian
Stage 10
Jiangshanian
Paibian
Guzhangian
Drumian
Wuliuan
Stage 4
Stage 3
Stage 2
Fortunian
Sponge reef ecosystem
Sponge reefs
~15 Ma
~5 Ma
E-M Cambrian mass extinction
Archaeocyath reef ecosystem
Mississippian
Late Devonian
Serpukhovian
Visean
Tournaisian
Famennian
Frasnian
Coral reef ecosystem
Bryozoan-coral reefs
~23 Ma
~12 Ma
Hangenberg mass extinction
Stromatoporoid reefs
F-F mass extinction
Stromatoporoid-coral reef ecosystem
Triassic
Permian
Late
Middle
Early
Lopingian
Norian
Carnian
Ladinian
Anisian
Olenekian
Induan
Changhsingian
Wuchiapingian
Coral-sponge -bivalve reef ecosystem
Sponge-coral -bivalve reef ecosystem
Sponge-bivalve -coral reefs
~9 Ma
~2 Ma
P-T mass extinction
Sponge-coral reef ecosystem

Fig. 11.

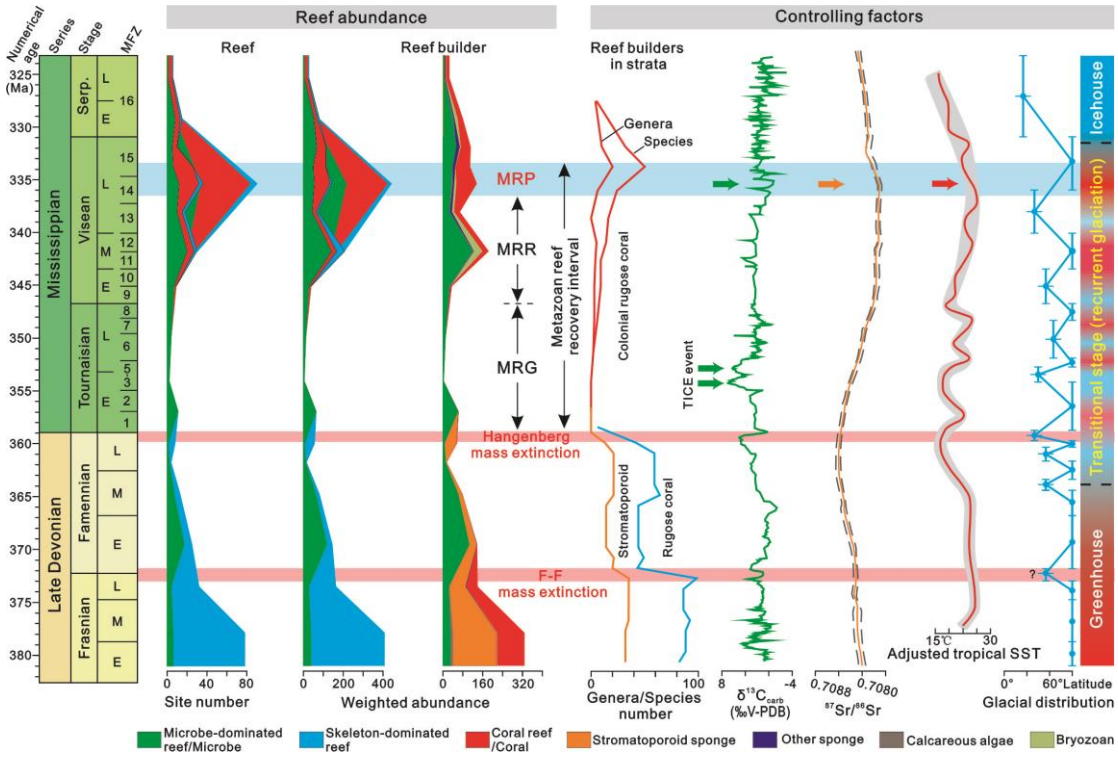
Numerical age (Ma)
Series
Stage
MFZ
Reef abundance
Controlling factors
Reef
Reef builder
Reef builders in strata
Mississippian
Late Devonian
Serp.
Visean
Tournaisian
Famennian
Frasnian
MRP
MRR
MRG
Metazoan reef recovery interval
Hangenberg mass extinction
F-F mass extinction
Genera
Species
Colonial rugose coral
TICE event
Stromatoporoid
Rugose coral
Adjusted tropical SST
Icehouse
Transitional stage (recurrent glaciation)
Greenhouse
Site number
Weighted abundance
Genera/Species number
δ13Ccarb (‰V-PDB)
87Sr/86Sr
Glacial distribution
Latitude
Microbe-dominated reef/Microbe
Skeleton-dominated reef
Coral reef /Coral
Stromatoporoid sponge
Other sponge
Calcareous algae
Bryozoan

Fig. 12